Clinical, splicing, and functional analysis to classify BRCA2 exon 3 variants: application of a points-based ACMG/AMP approach

Thomassen, M.; Mesman, R.L.S.; Hansen, T.V.O.; Menendez, M.; Rossing, M.; Esteban-Sanchez, A.; ... ; ENIGMA Consortium

Received: 12 November 2021 | Revised: 5 August 2022 | Accepted: 9 August 2022

DOI: 10.1002/humu.24449

RESEARCH ARTICLE

Human Mutation HGVS HUMAN GENOME VARIATION SOCIETY WILEY

Clinical, splicing, and functional analysis to classify *BRCA2* exon 3 variants: Application of a points-based ACMG/AMP approach

Mads Thomassen[1] | Romy L. S. Mesman[2] | Thomas V. O. Hansen[3] | Mireia Menendez[4] | Maria Rossing[5] | Ada Esteban-Sánchez[6] | Emma Tudini[7] | Therese Törngren[8] | Michael T. Parsons[7] | Inge S. Pedersen[9,10,11] | Soo H. Teo[12,13] | Torben A. Kruse[1] | Pål Møller[14] | Åke Borg[8] | Uffe B. Jensen[15] | Lise L. Christensen[16] | Christian F. Singer[17] | Daniela Muhr[17] | Marta Santamarina[18,19,20] | Rita Brandao[21] | Brage S. Andresen[22] | Bing-Jian Feng[23] | Daffodil Canson[7] | Marcy E. Richardson[24] | Rachid Karam[24] | Tina Pesaran[24] | Holly LaDuca[24] | Blair R. Conner[24] | Nelly Abualkheir[24] | Lily Hoang[24] | Fabienne M. G. R. Calléja[2] | Lesley Andrews[25] | Paul A. James[26,27] | Dave Bunyan[28] | Amanda Hamblett[29] | Paolo Radice[30] | David E. Goldgar[23] | Logan C. Walker[31] | Christoph Engel[32] | Kathleen B. M. Claes[33] | Eva Macháčková[34] | Diana Baralle[28] | Alessandra Viel[35] | Barbara Wappenschmidt[36,37] | Conxi Lazaro[4] | Ana Vega[18,19,20] | ENIGMA Consortium | Maaike P. G. Vreeswijk[2] | Miguel de la Hoya[6] | Amanda B. Spurdle[7]

[1]Department of Clinical Genetics, Odense University Hospital, Odence C, Denmark

[2]Department of Human Genetics, Leiden University Medical Center, Leiden, the Netherlands

[3]Department of Clinical Genetics, Rigshospitalet, Copenhagen University Hospital, Copenhagen, Denmark

[4]Hereditary Cancer Program, Catalan Institute of Oncology, ONCOBELL-IDIBELL-IDTP, CIBERONC, Hospitalet de Llobregat, Spain

[5]Center for Genomic Medicine, Rigshospitalet, Copenhagen University Hospital, Copenhagen, Denmark

[6]Molecular Oncology Laboratory, CIBERONC, Hospital Clinico San Carlos, IdISSC (Instituto de Investigación Sanitaria del Hospital Clínico San Carlos), Madrid, Spain

[7]Department of Genetics and Computational Biology, QIMR Berghofer Medical Research Institute, Brisbane, Queensland, Australia

[8]Division of Oncology, Department of Clinical Sciences Lund, Lund University, Lund, Sweden

[9]Molecular Diagnostics, Aalborg University Hospital, Aalborg, Denmark

[10]Clinical Cancer Research Center, Aalborg University Hospital, Aalborg, Denmark

[11]Department of Clinical Medicine, Aalborg University, Aalborg, Denmark

[12]Breast Cancer Research Programme, Cancer Research Malaysia, Subang Jaya, Selangor, Malaysia

[13]Department of Surgery, Faculty of Medicine, University of Malaya, Kuala Lumpur, Malaysia

Mads Thomassen and Romy L. S. Mesman should be considered joint first authors.

Maaike P. G. Vreeswijk, Miguel de la Hoya, and Amanda B. Spurdle should be considered joint senior authors.

[14]Department of Tumour Biology, The Norwegian Radium Hospital, Oslo University Hospital, Oslo, Norway

[15]Department of Clinical Genetics, Aarhus University Hospital, Aarhus N, Denmark

[16]Department of Molecular Medicine, Aarhus University Hospital, Aarhus, Denmark

[17]Department of OB/GYN and Comprehensive Cancer Center, Medical University of Vienna, Vienna, Austria

[18]Fundación Pública Galega de Medicina Xenómica, Santiago de Compostela, Spain

[19]Instituto de Investigación Sanitaria de Santiago de Compostela (IDIS), Complejo Hospitalario Universitario de Santiago, SERGAS, Santiago de Compostela, Spain

[20]Centro de Investigación en Red de Enfermedades Raras (CIBERER), Madrid, Spain

[21]Department of Clinical Genetics, Maastricht University Medical Center, Maastricht, the Netherlands

[22]Department of Biochemistry and Molecular Biology and the Villum Center for Bioanalytical Sciences, University of Southern Denmark, Odense, Denmark

[23]Department of Dermatology, Huntsman Cancer Institute, University of Utah School of Medicine, Salt Lake City, Utah, USA

[24]Ambry Genetics, Aliso Viejo, California, USA

[25]Hereditary Cancer Clinic, Nelune Comprehensive Cancer Care Centre, Sydney, New South Wales, Australia

[26]Parkville Familial Cancer Centre, Peter MacCallum Cancer Center, Melbourne, Victoria, Australia

[27]Sir Peter MacCallum Department of Oncology, The University of Melbourne, Melbourne, Victoria, Australia

[28]Human Development and Health, Faculty of Medicine, University of Southampton, Southampton, UK

[29]Middlesex Health Shoreline Cancer Center, Westbrook, Connecticut, USA

[30]Unit of Molecular Bases of Genetic Risk and Genetic Testing, Department of Research, Fondazione IRCCS Istituto Nazionale dei Tumori (INT), Milan, Italy

[31]Department of Pathology and Biomedical Science, University of Otago, Christchurch, New Zealand

[32]Institute for Medical Informatics, Statistics and Epidemiology, University of Leipzig, Leipzig, Germany

[33]Centre for Medical Genetics, Ghent University, Gent, Belgium

[34]Department of Cancer Epidemiology and Genetics, Masaryk Memorial Cancer Institute, Brno, Czech Republic

[35]Division of Functional Onco-genomics and Genetics, Centro di Riferimento Oncologico di Aviano (CRO), IRCCS, Aviano, Italy

[36]Center for Familial Breast and Ovarian Cancer, Faculty of Medicine and University Hospital Cologne, University of Cologne, Cologne, Germany

[37]Center for Integrated Oncology (CIO), Faculty of Medicine and University Hospital Cologne, University of Cologne, Cologne, Germany

Correspondence

Mads Thomassen, Department of Clinical Genetics, Odense University Hospital, Odence C 5000, Denmark.
Email: Mads.Thomassen@rsyd.dk

Amanda Spurdle, Department of Genetics and Computational Biology, QIMR Berghofer Medical Research Institute, Brisbane, QLD 4006, Australia.
Email: Amanda.Spurdle@qimrberghofer.edu.au

Funding information

Italian Ministry of Health; Den Norske Kreftforening; Spanish Health Research Foundation, Grant/Award Numbers: INT15/00070, INT16/00154, INT17/00133, INT20/000; NIHR Research Professorship, Grant/Award Number: RP-2016-07- 011; Ministry of Health of the Czech Republic MH CZ – DRO, Grant/Award Numbers: MMCI, 00209805 and NU20-03-00285; Federal Ministry of Education and Research, Grant/Award Number: 01GY1901; Government of Catalonia, Grant/Award Number: 2017SGR1282 and 2017SGR496; CERCA Program/ Generalitat de Catalunya and the Carlos III National Health Institute, Grant/Award Number: PI19/00553; PI16/00563; SAF2015-68016-R and CIBERO; German Cancer Aid, Grant/Award Number: 110837 and 70114178; Autonomous

Abstract

Skipping of *BRCA2* exon 3 (ΔE3) is a naturally occurring splicing event, complicating clinical classification of variants that may alter ΔE3 expression. This study used multiple evidence types to assess pathogenicity of 85 variants in/near *BRCA2* exon 3. Bioinformatically predicted spliceogenic variants underwent mRNA splicing analysis using minigenes and/or patient samples. ΔE3 was measured using quantitative analysis. A mouse embryonic stem cell (mESC) based assay was used to determine the impact of 18 variants on mRNA splicing and protein function. For each variant, population frequency, bioinformatic predictions, clinical data, and existing mRNA splicing and functional results were collated. Variant class was assigned using a gene-specific adaptation of ACMG/AMP guidelines, following a recently proposed points-based system. mRNA and mESC analysis combined identified six variants with transcript and/or functional profiles interpreted as loss of function. Cryptic splice site use for acceptor site variants generated a transcript encoding a shorter protein that retains activity. Overall, 69/85 (81%) variants were classified using the points-based approach. Our analysis shows the value of applying gene-specific ACMG/AMP guidelines using a points-based approach and highlights the consideration of cryptic splice site usage to appropriately assign PVS1 code strength.

Government of Galicia, Grant/Award Number: IN607B; Dutch Cancer Society KWF, Grant/Award Number: UL2012-5649 and Pink Ribbon-11704; NHMRC, Grant/Award Numbers: APP177524, APP1104808; Centro de Investigación Biomédica en Red de Enfermedades Raras CIBERER, Grant/Award Number: ACCI 2016: ER17P1AC7112/2018; Spanish Instituto de Salud Carlos III (ISCIII), Grant/Award Number: PI 20/00110; Fundación Mutua Madrileña

KEYWORDS
ACMG/AMP classification, *BRCA2*, dPCR, functional analysis, quantitation, splicing

1 | INTRODUCTION

Pathogenic variants in *BRCA2* predispose carriers to breast, ovarian, prostate, and other *BRCA2*-related cancers (Gayther et al., 1997). Although intensive gene testing has been performed for families with suspected hereditary cancer for more than 20 years, there are still considerable challenges for the interpretation of variants with uncertain clinical significance (Spurdle et al., 2012). Several naturally occurring alternative splice isoforms of *BRCA2* have been reported, and genetic variants have been shown to change the relative expression levels of these alternative transcripts (de Garibay et al., 2014; Fackenthal et al., 2016; Montalban et al., 2018). Interpretation of clinical significance for these spliceogenic variants is difficult as aberrant transcript expression patterns might impact protein function depending on both transcript ratios and the functional integrity of the alternative isoforms. Skipping of *BRCA2* exon 3 (ΔE3) is a naturally occurring in-frame splicing event (Peixoto et al., 2009; Thomassen et al., 2012). Several genetic variants have been shown to increase ΔE3 at the mRNA level (Caputo et al., 2018; Diez et al., 2007), and there is now convincing evidence that near exclusive expression of the ΔE3 transcript (also termed complete exon skipping, or complete ΔE3) is deleterious to protein function and confers high risk of *BRCA2*-related cancers (Caputo et al., 2018). The BRCA2 protein is, through interactions with several other proteins including BRCA1 and PALB2, involved in the repair of DNA double-strand breaks (DSBs) by homologous recombination (Sy et al., 2009). Exon 3 encodes the PALB2 interaction domain located at amino acids 21–39 (Oliver et al., 2009), and abrogation of BRCA2-PALB2 binding is the likely molecular mechanism underlying this increased risk (Hartford et al., 2016). In contrast, the *BRCA2* c.68-7T>A variant (Colombo et al., 2018) leads to moderately increased ΔE3 relative to wildtype (WT) levels (13% ΔE3, compared to 3% in non-carriers in lymphoblastoid cell line (LCL) cultures, inferring 23% ΔE3 expression from the A allele), but this variant is not associated with elevated breast cancer risk. A more recent analysis (Tubeuf et al., 2020) reported that a common synonymous variant c.231T>G rescued BRCA2 function in a mouse embryonic stem cell (mESC) complementation assay, with the G allele reported to exhibit 32%–40% ΔE3 in the mESC assay and 30% ΔE3 in a minigene assay. These findings suggested that moderately increased ΔE3 expression is not associated with high risk of cancer, complicating the clinical interpretation of variants that affect mRNA splicing in this region of the gene.

In this study, we assessed the pathogenicity of 85 variants located in or near *BRCA2* exon 3, using a variety of evidence types. These included new and existing data from mRNA and/or protein/cellular functional assays, frequency and bioinformatic data calibrated against clinical data, and additional likelihood-weighted clinical evidence. We show the value of applying gene-specific ACMG/AMP guidelines. In particular, this study provides real-world examples to demonstrate the flexibility of the recently proposed points-based approach (Tavtigian et al., 2020) to resolve variant interpretations.

2 | MATERIALS AND METHODS

The overall project, using deidentified data and laboratory results collated from multiple sites, was approved by the QIMR Berghofer Human Research Ethics Committee (Project 1051). Each participating site had Human Research Ethical Approval to cover use of patient material and data in research to evaluate variant pathogenicity, including: Ethical committee in Region of Southern Denmark and Capital Region of Denmark, approval VF20050011 and H-18058595, respectively (MT, MR); IdISSC/HCSC Ethics Committee, Project 15/139-E_BS and 21/308-E (MdelaH); Ethical committee of the Masaryk Memorial Cancer Institute (approval 2019/1845/MMCI: project NU20-03-00285) (EMA); IRB numbers EK-Nr 056/2005 and 2190/2019 from the Medical University of Vienna, IRB (CSI); The ethical committee at Lund University Dnr 2011/349 2011/652 (AB); Ethical Territorial Committee Research of Santiago Lugo, approval 2018/200 (AV); Ethics Committee of the University of Cologne (TEMP991529 and 19-1360_4) (BW); CRO Aviano, Local Ethical Committee, approval CRO-15-1997 (AVI) and IRB number IRAS ID 49685 (DB); Ethics committee of Bellvitge Biomedical Research Institute (IDIBELL; PR278/19) (MM). Use of the Ambry deidentified data set for research was deemed exempt from review by the Western Institutional Review Board.

2.1 | *BRCA2* exon 3 variants

A total of 89 variants were included in the study. Four previously classified variants with quantified splicing alterations were used as controls: Two variants were known to cause complete ΔE3 (Caputo

et al., 2018) and previously confirmed to be associated with *BRCA2*-related clinical phenotypes (c.156_157insAlu; c.316+5G>C); variant c.68-7T>A was included as a "partial skipping" control classified on the basis of clinical information as benign (Colombo et al., 2018); common synonymous variant c.231T>G, previously reported to exhibit at least 30% ΔE3 and also to rescue BRCA2 function in an mESC complementation assay (Tubeuf et al., 2020), was included as an mESC experimental control and was considered benign based on frequency. An additional variant was included as an experimental control: Variant c.316+5G>A, previously shown to lead to complete ΔE3 but not formally classified using clinical data (Caputo et al., 2018). Through examination of the literature, and/or by communication with ENIGMA members additional variants in exon 3 and the flanking introns were identified for inclusion in the study (Supporting Information: Table 1). For completeness, additional single nucleotide substitutions at the exon 3 acceptor site were included in minigene assays. In addition, four predicted missense substitution variants (c.91T>C p.(Trp31Arg), c.91T>G p.(Trp31Gly), c.93G>C p.(Trp31Cys), and c.93G>T p.(Trp31Cys)) were included in the mESC assay due to their location in the region relevant for BRCA2-PALB2 protein interaction (Oliver et al., 2009), and previous reports of variant impact on ΔE3 for c.93G>T (Biswas et al., 2012; Sanz et al., 2010; Sharan, personal communication).

Most variants had been identified in families with suspicion of hereditary breast and/or ovarian cancer. Overall, in addition to the controls with confirmed pathogenicity (pathogenic controls c.156_157insAlu, c.316+5G>C; benign controls c.68-7T>A and common synonymous variant c.231T>G), bioinformatic, mRNA, functional, and clinical data were collated for another 85 variants from the literature and/or as part of this study—including experimental control c.316+5G>A.

BRCA2 variants and alternative splicing events were described according to recommendations from the Human Genome Variant Society (HGVS) (http://varnomen.hgvs.org/), using as a reference the Refseq transcript NM_000059.3. For the sake of simplicity, we identified events as well with a code that combines the following symbols: Δ (skipping of reference exonic sequences), ▾ (inclusion of reference intronic sequences), p (acceptor shift), and q (donor shift). When necessary, the exact number of nucleotides skipped (or retained) is indicated.

Initial bioinformatic prediction to prioritize variants for mRNA assays was performed using MaxEntScan and ESEfinder software implemented in AlamutVisual 2.15 (https://www.interactive-biosoftware.com; Supporting Information: Table 1). See Section 2.3 for details on additional predictions used for comparison to mRNA findings and for variant interpretation.

2.2 | Laboratory analyses

Primers and methods used for mRNA assays are provided in Supporting Information: Table 2.

2.2.1 | Splicing analysis of patient samples and minigene assays

At study initiation, variants identified from ENIGMA collaborators to have bioinformatic prediction of altered splicing were prioritized for minigene assays and/or analysis of patient samples if available. Additional variants were included on the basis of mRNA availability only. Details on bioinformatics score and rationale for mRNA analysis are included in Supporting Information: Table 1. In total, excluding control variants, minigene assays were performed for 21 unique variants, and splicing assays on patient mRNA were performed across multiple labs for 14 unique variants. The patient samples were originally either sampled directly in RNA stabilizing agents (PAXgene® tubes and Tempus® tubes), or lymphocytes were grown as either short-term cultures or long-term EBV-transformed LCLs. To detect splicing alterations in addition to ΔE3 with high sensitivity, capillary gel electrophoresis was applied for 11 variants using methods described previously (de la Hoya et al., 2016). During the course of the study, published mRNA splicing results for these and additional variants in/near exon 3 were also collated.

2.2.2 | Quantitation of splice events by digital PCR

The use of digital PCR (dPCR) for precise quantification of *BRCA2* alternatively spliced isoforms has been described in detail elsewhere (Colombo et al., 2018). In brief, dPCR experiments were performed on a QuantStudio 3D dPCR 20K platform according to the manufacturer's instructions (Applied Biosystems). All quantification experiments were performed by combining FAM and VIC labeled TaqMan assays (Applied Biosystems) in individual chips. Chips were analyzed in the QuantStudio 3D Analysis Suit Cloud software v2.0 (Applied Biosystems), defining FAM as the target. Default settings were used in all cases. After reviewing the automatic assessment of the chip quality by the software, only green flag chips (data met all quality thresholds, review of the analysis result not required) and yellow flag chips (data met all quality thresholds, but manual inspection is recommended) were considered for further analyses. To detect *BRCA2* ΔE3, we used a FAM-labeled custom-designed TaqMan assay (Applied Biosystems) specific for the *BRCA2* exon 2-4 junction. *BRCA2* exon 3 retention was detected with a VIC-labeled Hs01556199 assay (Applied Biosystems) specific for the *BRCA2* exon 3-4 junction. ΔE3 level was calculated as exon 2-4/(exon 2-4 + exon 3-4). Note that, the latter assay will recognize different transcripts, provided that they have a native exon 3-4 junction, that is, the assay does not discriminate full-length expression from expression of transcripts with alterations at the exon 2-exon 3 junction, such as ΔE3p6 or ▾E3p2.

To better compare results using patient mRNA (where naturally occurring exon 3 skipping from the WT allele has to be accounted for) with data from assays measuring the effect of a single allele (i.e., minigene and mESC assay), the results were presented as absolute

ΔE3 level, and additionally as inferred per-allele ΔE3 level, calculated as follows: two times ΔE3 exclusion level observed in carriers minus the WT ΔE3 level (from same sample type).

Furthermore, the level of two other naturally occurring *BRCA2* alternative splicing isoforms (ΔE3-E4 and ΔE3-E7) skipping exon 3 (Fackenthal et al., 2016) were measured using FAM-labeled custom-designed TaqMan assay (Applied Biosystems) specific for the *BRCA2* exon 2-5 and exon 2-8 junctions, respectively. A full-length *BRCA2* transcript was detected with a VIC-labeled Hs00609073_m1 assay (Applied Biosystems) specific for the *BRCA2* exon 26-27 junction. Exclusion levels were calculated as exon 2-X/(exon 2-X + exon 26-27), where X refers to exon 5 or 8. Sequences of the Taqman probes are in Supporting Information: Table 2.

2.2.3 | RNA sequencing

Paired germline DNA-RNA genetic testing at Ambry Genetics, conducted on RNA isolated from blood collected in PaxGene tubes as described previously (Conner et al., 2019; Farber-Katz et al., 2018; Landrith et al., 2020), was performed for patients carrying *BRCA2* c.68-1G>A, c.68-2A>G and c.68-3T>G. Additional RNA-sequencing was performed to confirm the percent spliced in (PSI) of the observed transcripts, that is, exon–inclusion ratio. The SuperScript™ IV One-Step RT-PCR System (Thermo Fisher Scientific) was used to reverse transcribe and amplify 500 ng total RNA (see Supporting Information: Table 2 for details of primers). Thirty-five amplification cycles were performed with an annealing temperature of 52°C and a 45 s extension. Amplicons were purified using Ampure XP beads (Beckman Coulter) and quantified using the TapeStation D1000 system (Agilent). An input of 125 ng was used for preparation of Illumina dual indexed libraries using the Kapa HyperPrep kit with PCR (Roche), using 10 cycles of library amplification and a Covaris shearing protocol optimized to yield 300 bp fragments. Resulting libraries were pooled at equal molarities and sequenced using 150 bp paired-end reads on the Miseq platform (Illumina). A custom bioinformatics pipeline was used to align resulting reads and calculate PSI as described previously (Landrith et al., 2020).

2.2.4 | mESC functional assay

In this assay, variants are introduced in the full-length human *BRCA2* gene located on a Bacterial Artificial Chromosome (BAC) and subsequently transfected in a hemizygous mouse *Brca2* mESC line (Supporting Information: Figure 1) as described previously (Mesman et al., 2020). As BRCA2 protein activity is essential for mESC viability, the capacity of variants to rescue the lethal phenotype after removal of the conditional *mBrca2* allele can be used as a measure of variant protein function. Variants that severely impede cell viability are considered loss of function variants, while variants that rescue cell lethality to a certain extent can be characterized by their effect on homology-directed repair (HDR) in an additional functional assay. In a previous validation study, using variants of known pathogenicity as determined by multifactorial likelihood analysis (likely), pathogenic missense variants were either unable to rescue the lethal cell phenotype upon *mBrca2* loss or displayed an HDR level below 30% of WT BRCA2, while (likely) benign missense variants complemented the lethal phenotype and displayed HDR capacities between 50% and 120% of WT BRCA2 activity (Mesman et al., 2019). In this study, we introduced clone counting to stratify complementation categories.

The conditional *mBrca2* allele was removed by treating the cells with 1.0 μM 4-Hydroxytamoxifen (4-OHT; Sigma-Aldrich Merck KGaA) as described previously (Mesman et al., 2020). For each variant, the number of viable clones was compared to the complementation of WT BRCA2 expressing cells, and categorized in one of the following complementation categories: poor (<20% viability, including no complementation), reduced (20%–50% viability), or good (>50% viability). Variants in the last two categories were included in downstream functional analysis, using the DR-GFP reporter assay to measure variant capacity to repair an I-sce1 induced DSB, which leads to the restoration of a GFP gene construct (Mesman et al., 2020). The HDR activity for a variant was measured as the percentage of mCherry and GFP double-positive cells relative to the number of double-positive cells observed for WT BRCA2. For the DR-GFP reporter assay, all cell lines were seeded in triplicate, resulting in six GFP measurements per variant.

In addition to control variants c.68-7T>A, c.316+5G>C, and c.231T>G, 18 variants were selected for the mESC functional assay based on observation of increased ΔE3 or other aberrant splicing products detected by analysis of patient samples, minigene, or if the variant was predicted to (also) result in an amino acid change within the BRCA2-PALB2 interaction domain.

To study the effect of a variant on mRNA splicing, RNA was isolated from duplicate variant-expressing mESC using a TRIzol-based protocol. The dPCR method (described above) was applied on these RNA samples to analyze splicing patterns and quantify ΔE3 level. Capillary gel electrophoresis (described above) was also applied for variants c.68-2A>G and c.68-3T>G.

BRCA2 protein expression in BAC-transfected mESC was confirmed by western blot analysis using a rabbit polyclonal antibody (BETHYL, A303-434A-T) directed against a region between amino acids 450–500 in exon 10 of BRCA2, as described previously (Mesman et al., 2020).

2.3 | Variant classification

Variant classification was based on a gene-specific adaptation of the original ACMG/AMP guidelines (Richards et al., 2015), incorporating clinical, splicing, and functional information from multiple sources, and also bioinformatic-based and frequency-based codes with weights determined from empirical data. Requests were made to the ENIGMA membership via email for clinical information from variant carriers, including pedigree data and breast tumor histopathology status. Additional clinical, splicing, and functional data were sought from publications.

2.3.1 | Frequency-based codes

The applicable PM2 code strength was determined using the approach as described previously (Parsons et al., 2019). The likelihood ratio (LR) toward pathogenicity was estimated based on maximum population allele frequency for a set of 749 *BRCA1* and *BRCA2* variants that have previously been classified as (likely) benign or (likely) pathogenic using multifactorial likelihood analysis. All had MAF < 0.01 in a non-founder population; additionally, variants representing haplotype associations or large genomic rearrangements were excluded. Estimates were derived for the two genes combined, with the justification that they exhibit broadly similar penetrance and phenotype, and there would be greater confidence in estimates based on the larger sample size for the combined data set. Reference set variants were assigned to a frequency bin based on the maximum allele frequency observed in a non-founder sub-population (Non-Finnish European, African, Latino, East Asian, and South Asian), from gnomAD Version 2.1.1 (non-cancer) accessed 2020-07-20. The data set used for analysis is provided in Supporting Information: Table 3, and the details of LR estimation are shown in Supporting Information: Table 4. LR estimates were correlated with ACMG code strength as per Tavtigian et al. (2018).

An LR of 2.88 toward pathogenicity was estimated for the absence of a variant in gnomAD, indicating PM2_Supporting as the strength for this evidence type. In addition, the LR estimation of other frequency bins was used to determine cut-offs for BA1 (maximum allele frequency > 0.001) and BS1 (>0.0001 to 0.001). In addition, analysis indicated that maximum allele frequency from >0.00002 to 0.0001 could conservatively be used to assign supporting evidence against pathogenicity (BS1_Supporting).

Variants under study were assigned a relevant ACMG-based frequency code based on the maximum allele frequency in a non-founder sub-population (described as above).

2.3.2 | Bioinformatic-based codes

With respect to bioinformatic codes applied for potential spliceogenic variants, MaxEntScan (Yeo & Burge, 2004) scores in relation to native donor, native acceptor, and cryptic site usage were reviewed to assign splicing-related bioinformatic codes (see Supporting Information: Table 1 for descriptions). This included review of MaxEntScan-based categories for native donor/acceptor site loss and donor gain following cut-point recommendations of Shamsani et al. (2019), and additional consideration of MaxEntScan predictions of acceptor gain. The recommendations of Abou Tayoun et al. (2018) were considered to determine codes applicable for variants directly impacting the donor and acceptor sites. Exon 3 donor site changes are predicted to abrogate the site and lead to an in-frame event that deletes amino acids 23–105, which includes most of the PALB2 interaction domain, originally conservatively defined as amino acids 10–40 (Xia et al., 2006). Although this is an in-frame deletion of a single exon, it was considered appropriate to upgrade PVS1_Strong to PVS1 for donor site changes since variants leading to complete *BRCA2* ΔE3 have demonstrated clinical characteristics consistent with pathogenicity, for example, the LR in favor of pathogenicity based on segregation data for pathogenic control variant c.156_157insAlu was 6.41×10^{16} (Caputo et al., 2018). PVS1_Supporting was applied to single nucleotide substitution variants at the acceptor site, since the predicted effect was acceptor site abrogation and use of a nearby cryptic site to result in an aberrant transcript encoding a protein lacking two amino acids; the supporting code was assigned since the two amino acid deletion lies within the BRCA2-PALB2 interaction domain, and is bioinformatically predicted to impact protein function using BayesDel (see below).

Bioinformatic predictions (ESEfinder, RESCUE-ESE) for potential changes to Exonic Splice Enhancer or Silencer motifs (ESEs, ESSs) were recorded for comparison to splicing assay results, but not used to assign bioinformatic code. Similarly, variants were additionally reviewed for splicing-related predictions using the SpliceAI tool (Jaganathan et al., 2019), https://spliceailookup.broadinstitute.org, with the following parameters for each setting: genome version hg38, score type raw, max distance: 10,000 nt, Illumina's pre-computed scores yes, transcript NM_000059.4. Based on an analysis of previously published experimental and prediction data (Valenzuela-Palomo et al., 2022), SpliceAI predicted probabilities were assigned using a "two score" approach, whereby observation of two different scores >20% were considered predictive of leading to a splicing aberration. Namely, predicted exon 3 donor loss + exon 3 acceptor loss indicate predicted exon 3 skipping, predicted exon 3 donor loss + exon 3 (or intron 4) donor gain indicate predicted shorter (or longer) exon 3, predicted exon 3 donor loss + exon 4 acceptor loss indicates predicted intron retention, and so on. Conservatively, the lower of the two scores used to assign a given predicted splicing event was then used as the probability to lead to that predicted event. MES and SpliceAI predictions for consensus acceptor site variants are shown graphically in Supporting Information: Figure 2.

We used a combination of approaches to determine appropriate weights for bioinformatic codes for missense and in-frame indel variants. Substitution variants predicted (or shown) to alter splicing were excluded from data sets used for calibration. We first used heterogeneity analysis to determine the proportion of pathogenic variants considering location of these types of variants with respect to (likely) clinical important domains, and also in silico predicted the impact of the alteration at the protein level. Previous heterogeneity analyses (Easton et al., 2007; Li et al., 2020; Tavtigian et al., 2008) have shown convincingly that missense variation in toto does not contribute much to *BRCA1/2* related disease, and further that there is strong evidence against pathogenicity for missense variants outside of a key functional domain. For the purpose of missense variant calibration, key functional domains were previously defined as those which contain individual missense variants previously determined to be pathogenic using clinical data. We conducted heterogeneity analysis as described recently (Li et al., 2020), using the exact same data set, with the following alterations to the study design. In this analysis, we redefined the boundaries for known clinically important

functional domains, added the BRCA1 coiled-coiled domain as a potential clinically important domain (based on observation of Fanconi anemia-like abnormalities in mice homozygote for a coiled-coiled domain deletion (Nacson et al., 2020), and extended the calibration to compare results for BayesDel (NaN) to the A-GVGD prediction tool (http://agvgd.hci.utah.edu/) assessed in previous heterogeneity analyses. While both tools predict variant impact on protein function via missense substitutions, BayesDel has the capacity to additionally predict impact of in-frame indels. Briefly, we estimated the proportion of pathogenic variants in the data set that are likely to be clinically significant as a function of bioinformatically predicted classifications, and variant location in a domain (see Supporting Information: Table 5 for details, including definitions of domains). Results indicated that there is convincing evidence against pathogenicity for missense/in-frame protein alterations outside of a known clinically important domain: only 1% of variants in this category were estimated to be pathogenic (Supporting Information: Table 5). Stratification using BayesDel score identified few variants with predicted impact on protein function ($n = 42$, 2.7% of this subgroup, with only 7% of such variants predicted to be pathogenic based on clinical presentation). Further, for missense variants *within* the recognized clinically important functional domains, BayesDel had improved capacity to identify pathogenic variants over A-GVGD. For BayesDel Score ≥0.30, 83% of variants were estimated to be pathogenic, compared to 74% for A-GVGD. Note, we did not use the results from this analysis to formally derive LRs for ACMG code strength assignment, due to expectation of bias in the LR estimates. This clinically-generated data set was not annotated for missense variants previously determined to be benign on the basis of frequency or other information (since these are not reported clinically), and thus the overall proportion of variants annotated as (likely) pathogenic or VUS is likely higher than would be expected for a data set with complete annotation of missense variation.

We used the following approach to define LRs for pathogenicity. We reviewed the evidence for pathogenicity for *BRCA1* and *BRCA2* missense substitution variants by domain from a recent large-scale case–control study, including 60,466 breast cancer cases and 53,461 controls (Dorling et al., 2021). The results provided no evidence that missense variants located outside a domain were overall associated with increased risk, with risk estimates as follows: *BRCA1* OR 1.02 (0.94–1.10), *BRCA2* OR 0.97 (0.92–1.03). Given that case–control data may be used to provide strong evidence in favor of pathogenicity (ACMG/AMP code PS4), it seems logical to assert that these case–control findings provide strong evidence against pathogenicity for missense variants located outside of a protein domain. Indeed, this assertion is consistent with the results of an analysis of ClinGen submitter classifications for *BRCA1* and *BRCA2* variants according to protein domain (Dines et al., 2020), which provided evidence that variants in "coldspots" could be assigned a strong benign category based on their location alone.

For *BRCA1* and *BRCA2* missense substitution variants within a domain, we then estimated LRs for missense variants according to BayesDel score category, using functional impact as a surrogate for variant pathogenicity (Supporting Information: Table 6). Functional impact was assigned based on the aggregated results from nine studies (Supporting Information: Table 7). As above, variants known or predicted to alter splicing were excluded, as were variants with conflicting results between studies, since from our observation, these largely reflect experimental design issues that fail to capture mRNA aberrations. LRs were estimated separately for variants with no functional impact, partial impact, or complete impact. BayesDel score was not significantly predictive of partial impact on function. BayesDel score <0.3 was predictive of no impact on function, with derived LRs consistent with a Supporting Benign code. BayesDel score ≥0.3 was predictive of complete impact on function, with derived LRs consistent with a Moderate Pathogenic code. Considering also results from Supporting Information: Table 5, BayesDel categories <0.3 and ≥0.3 were conservatively considered as supporting evidence against (score <0.3) or toward (≥0.3) pathogenicity for missense variants within a domain.

None of the analyses denoted above estimated values for synonymous variants. However, the assumption is that silent variants (with no predicted impact on splicing) outside of a clinically important domain can be assigned the same Benign code strength as that for any missense alteration (with no predicted impact on splicing) outside of a clinically important domain, that is, BP7_Strong. Following the same logic, silent variants (with no predicted impact on splicing) located within a domain could be assigned the same evidence strength as missense variants with low predicted impact on function via effect on protein (BayesDel score <0.30). Further, since intronic variants outside of the consensus donor/acceptor motif (with no predicted impact on splicing) are commonly viewed as akin to synonymous variants, we suggest conservatively the assignment of a BP7_Moderate code, to recognize the limitations of bioinformatic tools in prediction of pseudoexonization (Canson et al., 2020).

We thus determined the following conservative recommendations for variants outside of the consensus sites, based on predictions using MaxEntScan for splicing, and BayesDel for missense/in-frame alterations:

- **PP3** for silent, intronic, or missense **variation predicted to alter splicing** (for exonic variants, irrespective of location in a domain)
- **PP3** for **missense variation within a key domain**, and predicted effect via missense alteration (BayesDel scores ≥0.30), having excluded possible impact on splicing.
- **BP4** for **missense variation within a key domain**, and low predicted effect via missense alteration (BayesDel scores <0.30), having excluded possible impact on splicing.
- **BP1_Strong** for **missense variation outside of a key domain**, having excluded possible impact on splicing.
- **BP7_Strong** for **synonymous variants located outside of a key domain**, having excluded possible impact on splicing.
- **BP7** for **synonymous variants located inside a key domain**, having excluded possible impact on splicing. Also apply for **intronic variants located within donor and acceptor motifs** (up to and including +8, −12 into the intron), and no predicted impact on splicing.

- **BP7_Moderate**. Apply for **intronic variants located outside of donor/acceptor motifs** (+9 or more, −13 or more), and no predicted impact on splicing.

The codes applied for each variant are noted in Supporting Information: Table 1. For this analysis restricted to *BRCA2* exon 3 variants only, key domain referred to the PALB2 interaction domain captured within exon 3, designated conservatively as amino acids 23–40 (Oliver et al., 2009; Xia et al., 2006). Predictions for BayesDel were annotated from Version 1 database (build date 2017-08-24), excluding allele frequency. For missense variants, BayesDel used a combination of individual deleteriousness scores including FATHMM, GERP++, LRT, Mutation Assessor, Mutation Taster, Polyphen2_HDIV, Polyphen2_HVAR, PROVEAN, SIFT, SiPhy_29way, VEST3, fitCons, fathmm-MKL coding, phastCons 100way, phastCons 20way, phyloP 100way, and phyloP 20way. For in-frame indels, BayesDel score is calculated using PROVEAN. An overview of the process for assigning bioinformatic codes is described in Section 3.

2.3.3 | Functional-based codes

Splicing data from this study and several publications were summarized to assess the clinical relevance of the result, accounting for assay method or RNA source. Intronic and synonymous variants with only ΔE3 observed, at a level similar to or below that seen for known benign variant *BRCA2* c.68-7T>A, were automatically designated to be of no clinical importance and code BS3 was assigned. We also reviewed the clinical data supporting variant assertions for variants assayed by Tubeuf et al. using mESC (Tubeuf et al., 2020), and *conservatively* extended BS3 code assignment to variants with up to 30% per-allele exon exclusion, either directly measured (mESC functional assay), or inferred (heterozygous samples). This conservative assignment was based on data for the common synonymous variant c.231T>G (maximum MAF > 1%), reported to demonstrate 30% ΔE3 in a minigene assay, and 32-40% ΔE3 and complementation of the null phenotype in an mESC assay (Tubeuf et al., 2020). Note, although results from the same study suggested a higher level of Δ E3 in LCL-derived mRNA (55%, ~85% inferred per-allele ΔE3 for the G allele), there was evidence for variability across repeats for this sample (Tubeuf et al., 2020), and review of experimental design and data for control variants c.68-7T>A revealed potential for preferential amplification of shorter ΔE3 fragments.

PS3 via effect on mRNA was assigned for near-complete ΔE3, defined as ≥90% ΔE3, based on previous observations for mini-gene results for variants with convincing clinical data supporting pathogenicity (Caputo et al., 2018). In instances where transcripts encoding small in-frame deletions were identified, no functional code was assigned unless results were available from the mESC assay that captured both mRNA and protein effects (see above). Based on calibrations against assay results reported in Mesman et al. (2019) for variants classified as (likely) pathogenic or (likely) benign against a model of high cancer risk (Parsons et al., 2019; Supporting Information: Tables 8 and 9), PS3 was assigned for variants which showed poor complementation in the mESC assay (<20% viability), and BS3 for variants with complementation and HDR activity >50%. In the absence of previous calibration data for variants with reduced complementation based on clone count (20%–50% viability), combined complementation and HDR were reviewed for the single variant with reduced complementation; given that HDR activity of 51% for c.316+6T>G variant falls at that bottom of the range for (likely) benign variants, the result was considered unclear, and no functional code was assigned. We also compared our findings for mESC assays to those of Tubeuf et al. (2020) for overlapping variants, summarized in Supporting Information: Table 10.

In summary, conservative application of functional-based codes was as follows:

- BS3 for intronic and synonymous variants with mRNA results detecting only ΔE3 at a level qualitatively determined to be similar to or below that seen for known benign variant *BRCA2* c.68-7T>A, or per-allele ΔE3 measured as up to 30%.
- BS3 for variants (intronic, synonymous, and missense) with complementation and HDR activity >50%, and no conflicting mESC results in the literature.
- PS3 for intronic and synonymous variants with near-complete ΔE3 (≥90% exon skipping).
- PS3 for variants (intronic, synonymous, and missense) which showed poor complementation in the mESC assay (<20% viability), and no conflicting mESC results in the literature.

For a small subset of predicted missense variants with no clinically relevant impact on splicing, results from functional studies were drawn from previous publications (Ikegami et al., 2020; Mesman et al., 2019), and assigned BS3 if reported to have no impact on function, or PS3 if reported to have impact on function.

2.3.4 | Clinical data codes

Bayes scores for segregation were derived as described previously (Thompson et al., 2003). Additional Bayes scores for segregation, derived using the same approach, were taken from previous publications (Caputo et al., 2018, 2021; Easton et al., 2007; Goldgar et al., 2004). In addition, the Bayes segregation score for c.93G>T p.(Trp31Cys) derived using a very similar method (Mohammadi et al., 2009), was extracted from Biswas et al.(2012). LRs for breast tumor pathology were applied according to Spurdle et al. (2014). LRs previously derived based on co-occurrence data (Easton et al., 2007) and personal and family history presentation (Caputo et al., 2021; Easton et al., 2007; Li et al., 2020) were also incorporated into the analysis. Segregation, pathology, co-occurrence, and personal/family history LRs were combined by multiplication to derive a combined odds towards causality (Goldgar et al., 2008). The combined clinical data was then assigned the relevant code strength based on "odds of

pathogenicity categories" arising from a Bayesian reanalysis of the ACMG/AMP variant classification guidelines (Tavtigian et al., 2018).

LR ranges for categories are summarized below:

- **Strong**: Benign <0.05–0.00285; Pathogenic >18.70–350
- **Moderate**: Benign <0.23–0.05; Pathogenic >4.30–18.70
- **Supporting**: Benign <0.48–0.23; Pathogenic >2.08–4.30
- **No evidence**: 0.48–2.08

The sources of information compiled for classification are detailed in Supporting Information: Table 1, with provenance of data collected as part of this study shown in Supporting Information: Table 11.

2.3.5 | Additional codes

The ACMG/AMP code PS1 is strong pathogenic evidence defined as "same amino acid change as a previously established pathogenic variant regardless of nucleotide change." This description was applied in the context of a variant outside of the consensus splice site with a similar predicted impact on mRNA splicing as another variant at that nucleotide position, for which the classification is determined to be pathogenic from **clinical** and other data (PS1 (Splicing)). The code was also applied conservatively at supporting level for variants already assigned a PVS1 code due to location at the consensus dinucleotide, and for which there was another variant located at the same consensus dinucleotide that was classified as pathogenic from **clinical** and other data (PS1 (Splicing)); this conservative approach prevents overweighting of a consensus site variant compared to the "original" pathogenic consensus site variant. The PS1 code was not applied for missense variants in this study, since there were no relevant variants for which it was applicable. We did not consider application of PM5, a missense substitution (with no predicted/known effect on mRNA splicing), located at a residue for which a pathogenic missense variant is known to occur, following the rationale that this code is more effectively captured by our clinically calibrated bioinformatic code combining domain and predicted missense effect. We also did not assign PM1, since our application of bioinformatic scores already accounted for domain.

2.3.6 | Combining criteria to derive final class

We first derived class using the original ACMG/AMP code combinations (Richards et al., 2015), following recommendations for minor changes in combinations arising from the Bayesian framework analysis of Tavtigian et al. (2018).

Then for comparison, codes were combined following the point system approach recently proposed to simplify scoring and class assignment (Tavtigian et al., 2020). Point values assigned for the different code strengths were as recommended in the original publication: Indeterminate=0; Supporting=1, Moderate=2, Strong=4, and Very Strong=8 for Pathogenic codes; negative values for Benign codes of same strength. Point ranges to assign class followed the conservative recommendations in the original publication: Benign ≤−7, Likely Benign −6 to −2, Uncertain −1 to 5, Likely Pathogenic 6–9, Pathogenic ≥10.

3 | RESULTS

A comprehensive summary of splicing, functional and clinical data, encapsulating data generated as part of this study and that from previous publications, is shown in Supporting Information: Table 1. Summary mRNA and/or functional data generated as part of this study (WT reference, four controls, and another 32 variants), together with a final classification based on combined evidence, is shown in Table 1. The sections below detail findings from analyses conducted as part of this study.

3.1 | mRNA transcript analysis using minigenes and patient samples

Details of mRNA results are shown in Supporting Information: Figure 3 (minigene results) and Supporting Information: Figure 4 (patient mRNA results), and findings are summarized in Table 1. Excluding control variants, minigene assays were performed for 21 unique variants, and splicing assays on patient mRNA were performed across multiple labs for 14 unique variants. Considering results from either approach, assay results for a total of 15 variants indicated that ΔE3 was at levels considered clinically unimportant (not detectable, at low levels comparable to WT, or similar to that of benign control c.68-7T>A), and there was no other impact on mRNA splicing.

Using qualitative comparisons to control variants, minigene or patient mRNA analysis showed three variants to exhibit ΔE3 at levels greater than that of benign control c.68-7T>A: c.68-3T>G, c.277_317-726delinsCCAT, and c.316+1G>T. Variant c.68-3T>G, predicted by MaxEntScan to inactivate the acceptor site (6.10->0), showed increased ΔE3 by minigene analysis. Complex variant c.277_317-726delinsCCAT deletes the donor site sequence, and analysis of mRNA from stabilized blood is concordant with previous analysis by Nordling et al. (1998) that the variant induces a high level of ΔE3. Donor site variant c.316+1G>T, previously shown to lead to complete ΔE3 by minigene assays (Caputo et al., 2018), was confirmed to show high levels of ΔE3 in mRNA from stabilized blood.

All variant substitutions impacting the native acceptor AG dinucleotide were predicted to abolish the acceptor site, and also to strongly increase the score for a cryptic splice site at position c.74 (2.17->7.77; Supporting Information: Figure 2). Minigene analysis showed evidence of slightly increased ΔE3 (for c.68-2A>G and c.68-1G>A), and use of the c.74 cryptic splice site as a major event; the latter major event was confirmed by sequencing of patient mRNA for c.68-2A>G (Supporting Information: Figures S3b and S4b). The mRNA transcript

TABLE 1 Summary of mRNA and/or functional studies conducted as part of this study[a]

			Patient RNA					mESC assay			Classification based on all information collated to date, using gene-specific ACMG/AMP criteria and points system approach
Variant	Protein	Minigene[b]	Splice assay using patient samples[b]	dPCR absolute exclusion rate[c]	dPCR inferred per-allele exclusion rate	RNA sequencing transcript proportions[d]	RNA sequencing inferred per-allele transcript proportions	dPCR absolute per-allele Δ(E3) exclusion rate[e]	Complementation Category[f] (clone viability: poor, <20%; reduced, 20%–50%; good, 50%)	HDR capacity (%)	See Supporting Information Table S1 for full details
WT	N/A	Reference	ΔE3↑ (Blood, Lymphocyte, LCL)	2.8% (Blood), 3.1% (Lymphocyte), 3.7% (LCLs)	N/A	Δ(E3) 2.7% (2.4%–3.0%) (Blood)	Δ(E3) 2.7% (2.4%–3.0%) (Blood)	6.1%	Reference	Reference	N/A
c.68-7T>A	p.?	ΔE3↑↑, 7% skipping reported in Caputo et al (PMID 29707112)	ΔE3↑↑, reported in Colombo et al. (PMID:29460995)	5.7% (Blood), 8.9% (Lymphocyte), 14.5% (LCLs)	8.7% (Blood), 14.7% (Lymphocyte), 25.2% (LCLs)			13.3%	Good	101	Partial skipping control—established Benign variant
c.156_157in-sAlu	p.?		ΔE3↑↑↑↑ (LCL)	52.3% (LCL)	100.0% (LCL)						Full skipping control—established Pathogenic Variant
c.316+5G>C	p.?	ΔE3↑↑↑↑, 95% exon skipping reported in Caputo et al (PMID 29707112)						99.1%	Poor	NA	Full skipping control—established Pathogenic variant
c.316+5G>A	p.?	ΔE3↑↑↑↑, 94% exon skipping reported in Caputo et al (PMID 29707112)	ΔE3↑↑↑↑ (Blood)	44.9% (Blood)	87.0% (Blood)						Full skipping control—confirmed as pathogenic based on ACMG/AMP approach, this study
c.231T>G	p.(=)							19.9%	Good	121	Partial skipping control—Benign control based on frequency, previous mESC results—selected as control for mESC assays in this study
c.68-7delT	p.?		ΔE3↑↑ (LCL)	4.9% (LCL)	6.0% (LCL)			2.5%	Good	81	Likely Benign

TABLE 1 (Continued)

Variant	Protein	Minigene[b]	Patient RNA: Splice assay using patient samples[b]	Patient RNA: dPCR absolute exclusion rate[c]	Patient RNA: dPCR inferred per-allele exclusion rate	Patient RNA: RNA sequencing transcript proportions[d]	Patient RNA: RNA sequencing inferred per-allele transcript proportions	mESC assay: dPCR absolute per-allele Δ(E3) exclusion rate[e]	mESC assay: Complementation Category[f] (clone viability: poor, <20%; reduced, 20%–50%; good, 50%)	mESC assay: HDR capacity (%)	Classification based on all information collated to date, using gene-specific ACMG/AMP criteria and points system approach: See Supporting Information Table S1 for full details
c.68-7dupT	p.?	ΔE3↑	Same as WT (Lymphocyte)	2.3% (Blood)	1.9% (Blood)			2.0%	Good	104	Benign
c.68-3T>G	p.?	ΔE3↑↑↑		16.3% (Lymphocyte)	29.7% (Lymphocyte)	Δ(E3), 20.4% (19.0%–21.9%); Δ(E3–E4), 2.4% (2.2%–2.6%); ▾(E3p2), 16.7% (14.5%–19.0%)	Δ(E3), 38.1 (35.2%–41.1%); Δ(E3–E4), 4.3% (4.0%–4.7%); ▾(E3p2), 33.4% (29.0%–37.8%).	9.9%	Good	90	Benign
c.68-2A>C	p.?	Δ(E3p6)									Uncertain
c.68-2A>T	p.?	Δ(E3p6)									Uncertain
c.68-2A>G	p.?	ΔE3↑, Δ(E3p6)	Δ(E3p6) (blood)	11.1% (Blood)	19.4% (Blood)	Δ(E3p6), 28.9% (26.0%–31.1%); Δ(E3), 8.2% (6.6%–10.2%)	Δ(E3p6), 57.9% (52.0%–62.2%); Δ(E3), 13.6% (10.4%–17.6%)	12.8%	Good	70	Likely Benign
c.68-1G>A	p.?	ΔE3↑, Δ(E3p6)				Δ(E3p6), 36.8%; Δ(E3), 7.9%	Δ(E3p6), 73.6%; Δ(E3), 13.2%				Uncertain
c.68-1G>C	p.?	Δ(E3p6)									Uncertain
c.68-1G>T	p.?	Δ(E3p6)									Uncertain
c.72_85delinsTTTAAA-TAGAT	p.(Leu24_-Leu29delin-sPheLeu-AsnArgPhe)		ΔE3↑↑, p.(Leu24_-Leu29delin-sPheLeuAs-nArgPhe) (LCL)	26.4% (LCL), 12.0% (Blood)	49.2% (LCL), 20.8% (Blood)			23.5%	Poor	NA	Pathogenic
c.79A>G	p.(Ile27Val)	ΔE3↑						2.0%	Good	107	Likely Benign
c.91T>C	p.(Trp31Arg)	ΔE3↑↑	Same as WT (Lymphocytes)	10.1% (Lymphocyte)	17.1% (Lymphocyte)			9.5%	Poor	NA	Likely Pathogenic
c.91T>G	p.(Trp31Gly)							12.0%	Poor	NA	Uncertain
c.93G>C	p.(Trp31Cys)	ΔE3↑↑						10.5%	Poor	NA	Uncertain
c.93G>T	p.(Trp31Cys)							23.3%	Poor	NA	Uncertain

(Continues)

TABLE 1 (Continued)

Variant	Protein	Minigene[b]	Patient RNA: Splice assay using patient samples[b]	Patient RNA: dPCR absolute exclusion rate[c]	Patient RNA: dPCR inferred per-allele exclusion rate	Patient RNA: RNA sequencing transcript proportions[d]	Patient RNA: RNA sequencing inferred per-allele transcript proportions	mESC assay: dPCR absolute per-allele Δ(E3) exclusion rate[e]	mESC assay: Complementation Category[f] (clone viability: poor, <20%; reduced, 20%–50%; good, 50%)	mESC assay: HDR capacity (%)	Classification based on all information collated to date, using gene-specific ACMG/AMP criteria and points system approach: See Supporting Information Table S1 for full details
c.102A>G	p.(=)							35.0%	Good	89	Likely Benign
c.116C>T	p.(Ala39Val)	Same as WT	Same as WT (Blood)	6.6% (Blood)	10.4% (Blood)			2.1%	Good	72	Benign
c.125A>G	p.(Tyr42Cys)	Same as WT	Same as WT (Lymphocytes)	5.0% (Lymphocyte)	6.9% (Lymphocyte)						Benign
c.167A>C	p.(Asn56Thr)	Ssame as WT									Benign
c.179A>G	p.(Asn60Ser)	Same as WT									Benign
c.198A>G	p.(=)	Same as WT	Same as WT (Lymphocytes)	6.0% (Lymphocyte)	8.9% (Lymphocyte)						Benign
c.223G>C	p.(Ala75Pro)	Same as WT	Same as WT (Blood, LCL)	5.9% (Lymphocyte)	8.7% (Lymphocyte)						Benign
c.226T>C	p.(Ser76Pro)	ΔE3↑									Likely Benign
c.241T>C	p.(Phe81Ile)	Same as WT						0.6%	Good	72	Benign
c.277_317-726de-linsCCAT	p.?		ΔE3↑↑↑↑ (Blood)	28.7% (Blood)	54.6% (Blood)						Pathogenic
c.280C>T	p.(Pro94Ser)		Same as WT (LCL)	3.5% (LCL)	3.3% (LCL)			1.5%	Good	98	Benign
c.316+1G>T	p.?	ΔE3↑↑↑↑, complete skipping also reported in Caputo et al (PMID: 29707112)	ΔE3↑↑↑↑ (Lymphocytes)	40.4% (Blood) 55.0% (Lymphocyte)	77.9% (Blood) 107.9% (Lymphocyte)			99.7%	Poor	NA	Pathogenic
c.316+6T>A	p.?							82.6%	Good	60	Uncertain
c.316+6T>G	p.?							80.4%	Reduced	51	Uncertain

TABLE 1 (Continued)

Variant	Protein	Minigene[b]	Patient RNA: Splice assay using patient samples[b]	Patient RNA: dPCR absolute exclusion rate[c]	Patient RNA: dPCR inferred per-allele exclusion rate	Patient RNA: RNA sequencing transcript proportions[d]	Patient RNA: RNA sequencing inferred per-allele transcript proportions	mESC assay: dPCR absolute per-allele Δ(E3) exclusion rate[e]	mESC assay: Complementation Category[f] (clone viability: poor, <20%; reduced, 20%–50%; good, 50%)	mESC assay: HDR capacity (%)	Classification based on all information collated to date, using gene-specific ACMG/AMP criteria and points system approach: See Supporting Information Table S1 for full details
c.316+6T>C	p.?							56.3%	Good	82	Likely Benign
c.316+65A>G	p.?	ΔE3↑↑	Same as WT (LCL)								Likely Benign

[a]Light gray highlighted cell indicates not assayed in this study, for the relevant column. Control samples are in bold. Transcript notations are as follows:▾(E3p2) r.67_68ins68-2_68-1 p.(Asp23Glufs*3); Δ(E3p6) r.68_73del p.(Asp23_Leu24del); **Δ**(E3) r.68_316del p.(Asp23_Leu105del); ΔE3-E4 r.68_425del p.(Asp23Valfs*10).

[b]Key to result description: Same as WT—either no skipping, or skipping consistent with WT control/s for assay type; ΔE)↑: extremely low exon skipping detected by visual inspection but considered greater than WT control variant; ΔE3↑↑: Less than ~10% exon skipping detected by visual inspection; ΔE3↑↑↑ exon skipping >10% but considered incomplete by visual inspection; ΔE3↑↑↑↑ (almost) complete skipping. # note that in addition to ΔE3↑↑, the variant allele produces an altered full-length transcript r.72_85delinsTTTAAATAGAT p.(Leu24_Leu29delinsPheLeuAsnArgPhe). Multi-exon exclusion was measured by dPCR on patient-derived mRNA for control variants and c.315+1G>T (see Supporting Information: Figure S4), and was found to occur at negligible levels. *Note*: Assay on patient mRNA for c.68-2A>G was designed to capture only acceptor site usage, and could not capture upregulation of exon 3 skipping.

[c]Blood, directly stabilized blood; LCL, lymphoblastoid cell line; lymphocyte, short-term lymphocyte culture.

[d]Details listed for alternative transcripts comprising at least 2% of the overall profile. See Supporting Information: Figure S5a for further details about other minor transcripts reported.

[e]Additional notes regarding transcripts detected by capillary electrophoresis (Supporting Information: Figure S7): For variant c. 68-3T>G, 10% ΔE3 transcript was expressed relative to full-length plus ▾(E3p2) transcripts. For variant c.68-2A>G, no full-length transcript was detected, only exon skipping and a 6bp deletion transcript consistent with predicted cryptic site usage; 13% ΔE3 transcript was expressed relative to Δ(E3p6) transcript (r.68_73del).

[f]Complementation categories were defined based on clone viability relative to wildtype (WT), as follows: poor (<20% viability), reduced (20%–50% viability), and good (>50% viability). Blue font: exon 3 exclusion at levels considered clinically unimportant (if no other impact on mRNA splicing), including: not detectable, at low levels comparable to WT, similar to that of benign control c.68-7T>A, or estimated from quantitative studies to be at or below 30% inferred per-allele ΔE3).

arising from use of the cryptic splice site Δ(E3p6) encodes an in-frame deletion of two amino acids, p.Asp23_Leu24del. Minigene assays supported use of c.74 for five additional single nucleotide substitutions at the splice site, with a slight increase in ΔE3 observed for c.68-1G>A (Supporting Information: Figure S3b, Table 1).

Variant c.72_85delinsTTTAAATAGAT was not predicted to alter the WT acceptor (MaxEnt score 6.10), but a new predicted acceptor sequence (MaxEnt score 3.33) is introduced in the inserted sequence. Splice assays for c.72_85delinsTTTAAATAGAT using LCL and PAXgene® mRNA provided no evidence for usage of the de novo acceptor site, with use of the WT acceptor site in addition to ΔE3 levels in the broad range (or higher depending on sample type) observed for benign control c.68-7T>A (Figure 1, Supporting Information: Figure S4a). The resulting mRNA transcript encodes a protein with deletion of six amino acids and insertion of five new amino acids p.(Leu24_Leu29delinsPheLeuAsnArgPhe).

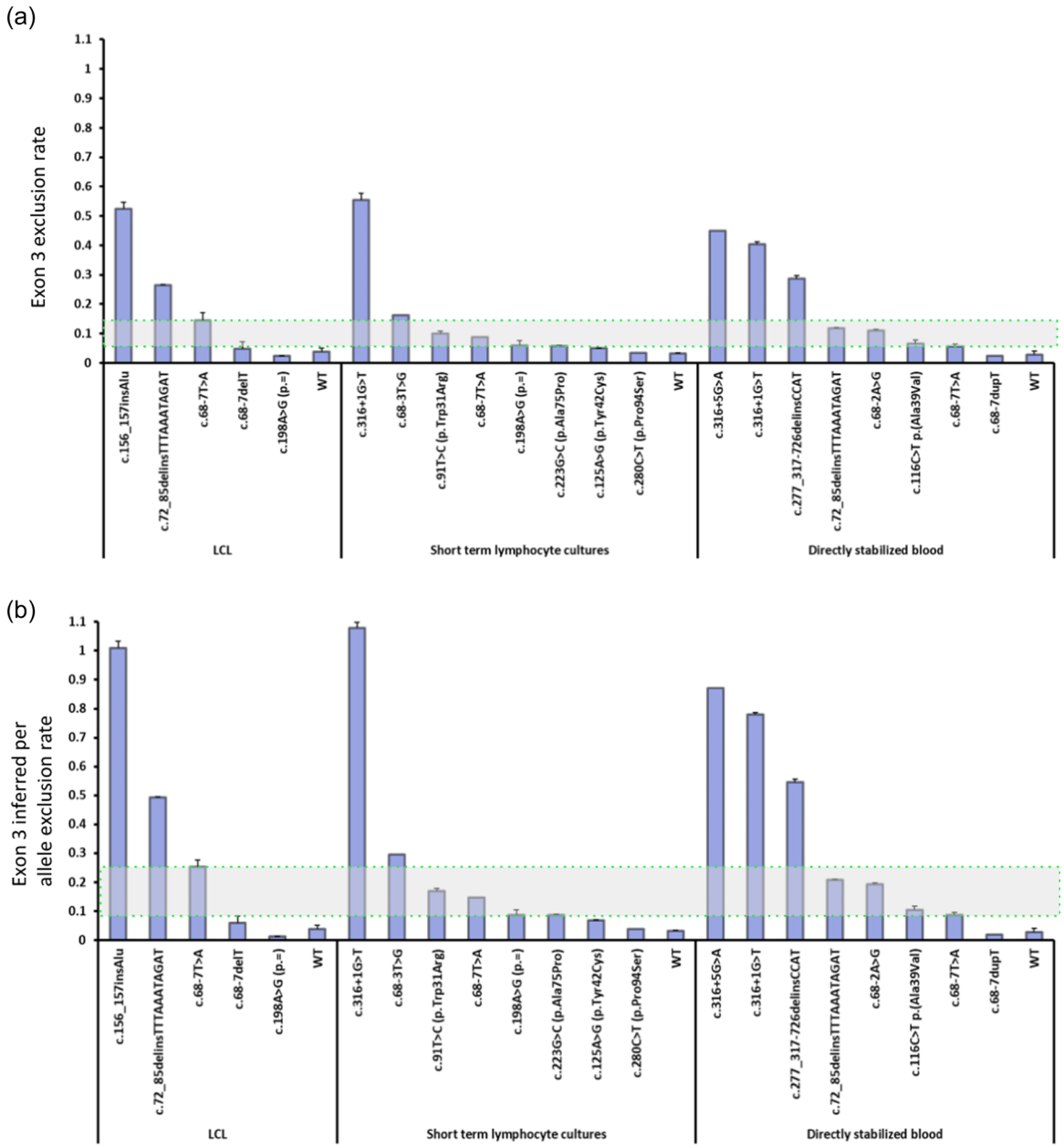

FIGURE 1 Quantitative dPCR of ΔE3 in patient samples. (a) Measured (absolute) ΔE3 rate. (b) Inferred per-allele ΔE3 rate. See Section 2 for details about ΔE3 rate calculations. Three different sample types were analyzed: lymphoblastoid cell line (LCL) cultures, short-term lymphocyte cultures, and directly stabilized blood (Paxgene, Tempus, and Trizol). Mean values and standard deviation for at least two replicates for each variant are shown. Complete ΔE3 variant controls are c.156_157insAlu and c.316+5G>A. The ΔE3 rate interval for known benign variant c.68-7T>A is shown as a horizontal green bar, defined by the lower boundary observed for RNA from directly stabilized blood and the upper boundary observed for RNA from LCL culture.

3.2 | ΔE3 level quantification by dPCR in patient-derived RNA samples

dPCR on 16 patient-derived RNA samples was performed to more accurately quantify exon 3 exclusion. In particular, this was necessary to compare ΔE3 level observed for individual variants to that observed for known pathogenic or benign control variants known to lead to ΔE3. Depending on sample type (directly stabilized blood, short-term cultures, or LCLs), dPCR analysis showed absolute exclusion levels of 5.7%-14.5% for the benign "partial" skipping control c.68-7T>A sample, while absolute exclusion levels for the complete ΔE3 control variants ranged from 44.9% (c.316+5G>A; blood) to 52.3% (c.156_157insAlu; LCL; Figure 1a). The inferred *per-allele* ΔE3 levels for the c.68-7A allele (Figure 1b, Table 1) were 8.7% (blood), 14.7% (lymphocyte), and 25.2% (LCLs), with per-allele exclusion for "complete ΔE3" variant controls ranging from 87.0% (c.316+5G>A; blood) to 100.0% (c.156_157insAlu; LCL).

To investigate the impact of previously reported naturally occurring multi-exon skipping transcripts, we analyzed ΔE3-E4 and ΔE3-E7 for full exon 3 skipping variants c.316+1G>T and c.316+5G>A, and benign control c.68-7T>A. Very low exclusion levels (i.e., lower than 3% in all cases) for the multi-exon skipping transcripts were observed across multiple tissue types (Supporting Information: Figure 5).

3.3 | RNA sequencing analysis of patient-derived RNA samples

RNAseq analysis was performed in c.68-3T>G ($N = 2$), c.68-2A>G ($N = 5$), and c.68-1G>A ($N = 1$) carriers, as well as in control samples ($N = 2$; Supporting Information: Figure 6). In c.68-3 T>G carriers, ΔE3 (20.4% of reads; range 19.0%–21.9%) and ▾E3p2 (16.7%; range 14.5%–19.0%) were the predominant aberrant transcripts. In c.68-2A>G and c.68-1G>A carriers, the predominant aberrant transcripts were ΔE3p6 (28.9%; 26.0%–31.1% and 36.8%, respectively) and ΔE3 (8.2%; 6.6%–10.2% and 7.9%, respectively). Control samples expressed ΔE3 at low levels (2.7%; 2.4%–3.0%). Table 1 and Figure 2 show the corresponding inferred per-allele expression levels. RNAseq detected other transcripts both in controls and variant carriers (including ΔE3-E4), although at very low levels (i.e., less than 3%).

3.4 | Inferred clinical relevance of splicing patterns

For the interpretation of variants, we reasoned that the effect on mRNA splicing will *not* have a significant clinical impact for any variant with a per-allele ΔE3 level similar or lower than observed for c.68-7T>A, if no other alternative splicing events are detected. Taking into account mRNA sample source, this deduction could be applied for seven variants in the study: c.68-7delT, c.68-7dupT,

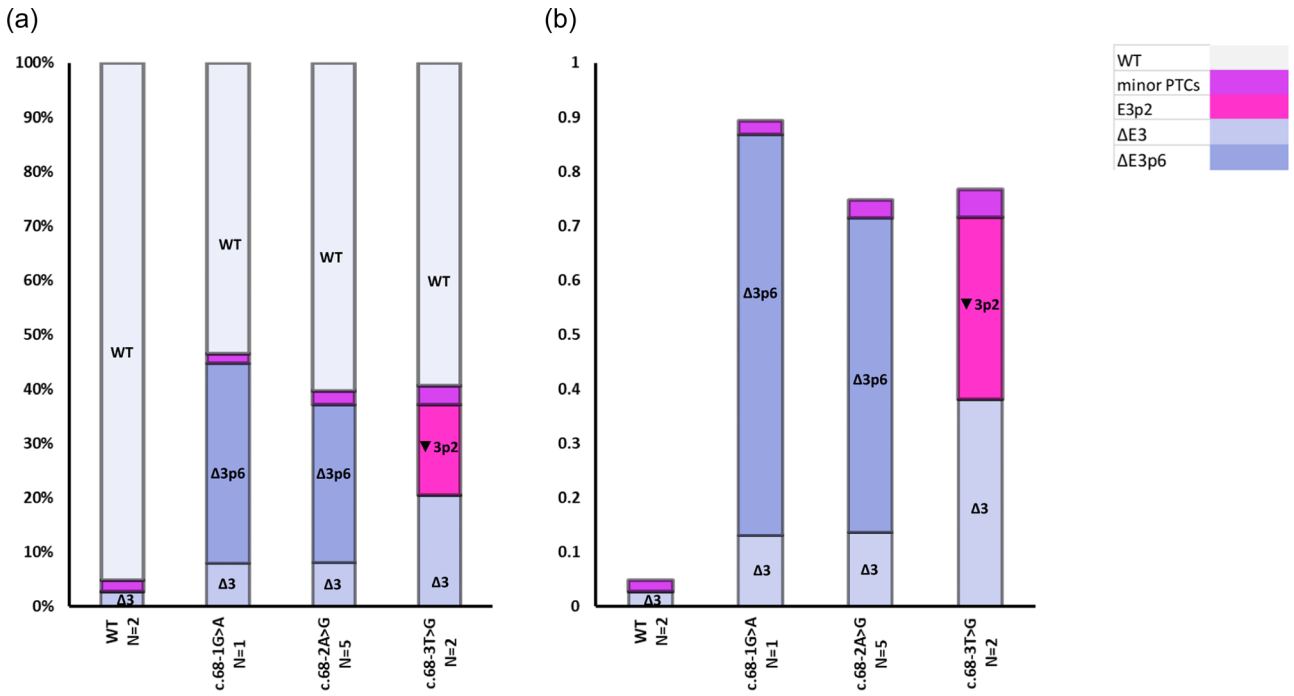

FIGURE 2 Quantitative RNA sequencing of patient RNA samples. (a) Relative contribution of transcripts (expressed as a proportion of total 100%). (b) The bars show inferred per-allele expression relative to total transcript amount. A number of low expressed transcripts expected to encode a protein termination codon (PTC) are summarized as minor PTCs. More detailed information, including standard deviation measures, is available in Supporting Information: Figure S6a. N = number of individuals assayed.

c.116C>T, c.125A>G, c.198A>G, c.223G>C, and c.280C>T (Table 1). The combination of minigene data (Supporting Information: Figure S3c), patient assay results (Supporting Information: Figure S4i), and dPCR inferred per-allele ΔE3 level (17.1%, Figure 1b) for c.91T>C, suggested at best a modest increase in ΔE3 for this variant. ΔE3 was slightly increased above that of c.68-7T>A for variant c.68-3T>G (29.7%) (Figure 1b, Table 1), with per-allele ΔE3 level using RNA-sequencing methodology of 38.1% (Figure 2).

The clinical interpretation of splicing results was less clear for the following variants, due to the somewhat increased levels of ΔE3 relative to WT controls, presence of additional aberrant (in-frame or other) transcripts, and/or ability of the variant-induced mRNA transcript to encode a protein with an in-frame alteration in amino acid sequence. Variants c.68-2A>G and complex deletion–insertion variant c.72_85delinsTTTAAATAGAT displayed a more complex mRNA transcript pattern, including different aberrant in-frame transcripts (Supporting Information: Figure S4a,b) in combination with increased ΔE3. Inferred per-allele ΔE3 levels for c.68-2A>G were 19.4% (blood), and for c.72_85delinsTTTAAATAGAT were 20.8% (blood) and 49.2% (LCL). Results for c.68-2A>G were similar by RNA-sequencing, with average 57.9% inferred per-allele expression of a transcript encoding p.Asp23_Leu24del, in addition to average 13.6% inferred per-allele expression of ΔE3 (Figure 2). Variant c.277_317-726delinsCCAT displayed a greater proportion of ΔE3, with dPCR per-allele ΔE3 level of 54.6% in patient mRNA from stabilized blood (Figure 1).

Variant c.316+1G>T displayed extensive ΔE3 relative to controls (inferred per-allele 79% in patient mRNA from stabilized blood, >100% in mRNA from short-term lymphocyte culture), consistent with a severe impact on the exon 3 donor site.

3.5 | Functional characterization of *BRCA2* exon 3 region variants using an mESC-based assay

To directly assess the functional impact of variant-induced ΔE3 and/or effect on protein via change in amino acid sequence, we utilized an mESC assay validated against known pathogenic and benign missense variants (see Section 2). Wild-type *hBRCA2*, benign control variants c.68-7T>A and c.231T>G, pathogenic control variant c.316+5G>C, and another 18 *BRCA2* gene variants were transfected into hemizygous mESC.

3.5.1 | Analysis of ΔE3 level in mESC-derived RNA samples

Variants c.316+1G>T and c.316+5G>C showed near complete exon 3 skipping (99.7% and 99.1% ΔE3, respectively) in mESC-derived mRNA (Supporting Information: Figure S7). Variants c.316+6T>A and c.316+6T>G displayed severely increased ΔE3 transcript levels (80%), while c.316+6T>C displayed a more moderate level of ΔE3 (56%). For synonymous variants c.102A>G and c.231T>G, ΔE3 levels were 35% and 20%, respectively. The ΔE3 level for c.68-2A>G (12.8%) and c.68-3T>G (9.9%) was comparable to the ΔE3 level observed for benign variant c.68-7T>A (13.3%). For c.72_85delinsTTTAAATAGAT ΔE3 level was approximately double (23.5%) that observed for c.68-7T>A. For the other variants, ΔE3 was either not detected, or detected as a minor event at levels below that observed for c.68-7T>A. Capillary electrophoresis of RNA for variant c.68-2A>G (Supporting Information: Figure S8) confirmed expression of the transcript lacking six bases (ΔE3p6) in addition to ΔE3. As summarized in Supporting Information: Table 10, overall trends in observed mESC splice patterns from assays in this study (Table 1), were in line with those previously published (Tubeuf et al., 2020), considering differences in experimental design that have previously been shown to overestimate levels of the smaller ΔE3 products (Colombo et al., 2018). As expected, the absolute per-allele ΔE3 level from dPCR analysis (this study) was consistently lower than that measured using semi-quantitative RT-PCR (Tubeuf et al., 2020), and differences were more marked for samples/variants with lower ΔE3 (WT control, c.102A>G, c.231T>G). Despite this, the bioinformatically predicted probability of exon exclusion for the three variants at the +6 position appeared to correlate with within-study relative levels of ΔE3 expression.

3.5.2 | The functional impact of BRCA2 exon 3 variants

Complementation phenotype, the ability of variants to rescue the lethal cell phenotype upon *mBrca2* loss, is shown in Supporting Information: Figure S9. Confirmation of protein expression is shown in Supporting Information: Figure S10. Poor complementation, indicative of loss of protein function, was observed for the pathogenic control c.316+5G>C, variant c.316+1G>T known to lead to (near) complete ΔE3, and another five variants (c.72_85delinsTTTAAATAGAT, c.91T>C, c.91T>G, c.93G>C; c.93G>T). Variant c.316+6T>G displayed reduced complementation (20%–50% viability), and all other variants revealed a good complementation capacity (>50% viability relative to WT).

The 14 variants (including benign control variant c.68-7T>A) with reduced or good complementation (Supporting Information: Figure S9), were assessed for HDR capacity (Figure 3). All variants demonstrated HDR activity above 50%, in the range previously observed for variants classified as (likely) benign using multifactorial likelihood analysis approaches. Notably, variant c.316+6T>G with reduced complementation displayed 51% HDR, just above the lower boundary previously defined for BRCA2 missense variants classified as (likely) benign using multifactorial likelihood approaches (Mesman et al., 2019).

As shown in Supporting Information: Table 10, mESC complementation and secondary analysis results were also compared to those reported for overlapping variants assayed using related methodology by Tubeuf et al. (2020). This revealed apparent differences in results for the c.316+6T>A and c.316+6T>G variants,

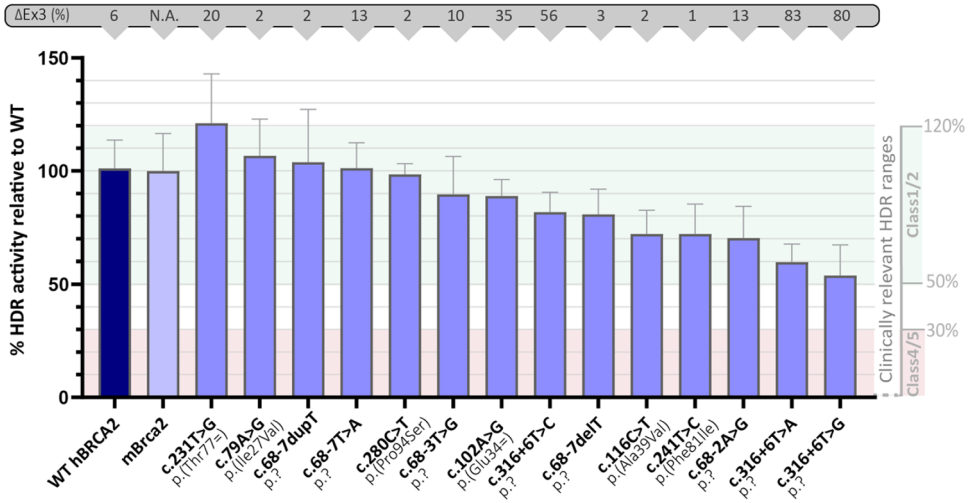

FIGURE 3 HDR activity of *BRCA2* exon 3 variants in mESC. The fraction of GFP-expressing cells was determined by flow cytometry 2 days posttransfection with an I-Sce1 expression vector. *mBrca2* represents the conditional *Brca2*$^{-/loxP}$; Pim1$^{DR\text{-}GFP/WT}$ cell line expressing endogenous mouse *Brca2*. The upper green box represents the HDR range previously reported for Class 1/2 *BRCA2* variants (classified as (likely) benign using multifactorial likelihood analysis). The lower red box represents the HDR range reported to be associated with >95% probability of pathogenicity (Guidugli et al., 2018), and used to define a pathogenic HDR range for the mESC assay (Mesman et al., 2019). Error bars indicate the SD of at least six independent GFP measurements per variant. The upper gray bar indicates the ΔE3 levels as measured by quantitative dPCR (E2E4 junctions vs. E3E4 junctions) using RNA samples isolated from variant-expressing mESC. Note that E3E4 junction captures full-length expression, but also expression of ▾E3p2 and ΔE3p6 transcripts (as observed respectively, in c.68-3T>G and c.68-2A>G mESCs). HDR, homology-directed repair; mESC, mouse embryonic stem cell.

complicated by differences in viability thresholds used to assign complementation categories and differences in secondary analysis approaches. Given that the level of ΔE3 (as measured by either study) fell outside the range set for assigning PS3 or BS3, no functional code was assigned for these two variants. Results for variant c.316+6T>C were consistent across the two studies (good complementation).

3.6 | Classification of variants using a gene-specific adaptation of the ACMG/AMP criteria

This study included analysis of four control variants classified with respect to pathogenicity (benign controls c.68-7T>A, c.231T>G; pathogenic controls c.156_157insAlu, c.316+5G>C), complete ΔE3 experimental control c.316+5G>T, and another 84 variants from the *BRCA2* exon 3 region. Clinical, splicing, and functional data collected for this study, or derived from previous publications, were used to assign a classification following a gene-specific adaptation of the ACMG/AMP criteria (see Section 2 for details; of necessity, the PVS1 codes derived are for exon 3 donor and acceptor only, and applicable at the level of exon). Figure 4 provides an overview of the application of codes relating to variant position and bioinformatic prediction of effect, and subsequent interpretation and code application relating to mRNA and functional data.

Specifically, classification categories were assigned using the points-based ACMG/AMP system, allowing the application of additional LR-based benign code strengths for clinical data, and a greater range of options to combine benign and pathogenic data points compared to the code-combinations originally proposed (Richards et al., 2015; Tavtigian et al., 2020). The breakdown of variant classifications using the points-based approach was as follows: 31 Benign, 32 Likely Benign, 16 Uncertain, 2 Likely Pathogenic, and 4 Pathogenic (Supporting Information: Table 1). For 1 Likely Pathogenic, 11 Benign, and 26 Likely Benign points-based variant classifications, classifications were at a lower confidence level or uncertain using the original code combinations. Of the four variants classified as Pathogenic, one was the complete skipping experimental control c.316+5G>A, another two also led to complete exon 3 skipping (c.277_317-726delinsCCAT, c.316+1G>T), and the other was the complex deletion–insertion variant c.72_85delinsTTTAAATAGAT which led to an in-frame change in protein sequence predicted bioinformatically to impact function. The Likely Pathogenic classifications for variants c.91T>C p.(Trp31Arg) and c.92G>C p.(Trp31Ser) were driven by direct and/or clinical evidence of functional impact via the missense change, since there was no evidence for altered splicing for either variant.

Of interest is that the exon 3 acceptor site variants were assigned a low bioinformatic code of PVS1_Supporting due to MaxEntScan-predicted use of a cryptic acceptor site resulting in an aberrant transcript encoding a two amino acid deletion (Table 1). We note that the more recently developed SpliceAI tool also predicted high probability of using the cryptic splice site (>95%) for all six single nucleotide substitutions (Supporting Information: Figure 2). The assigned conservative annotation for this acceptor site was justified by observations from splicing and functional assay results. All six acceptor site variants were confirmed to induce this in-frame

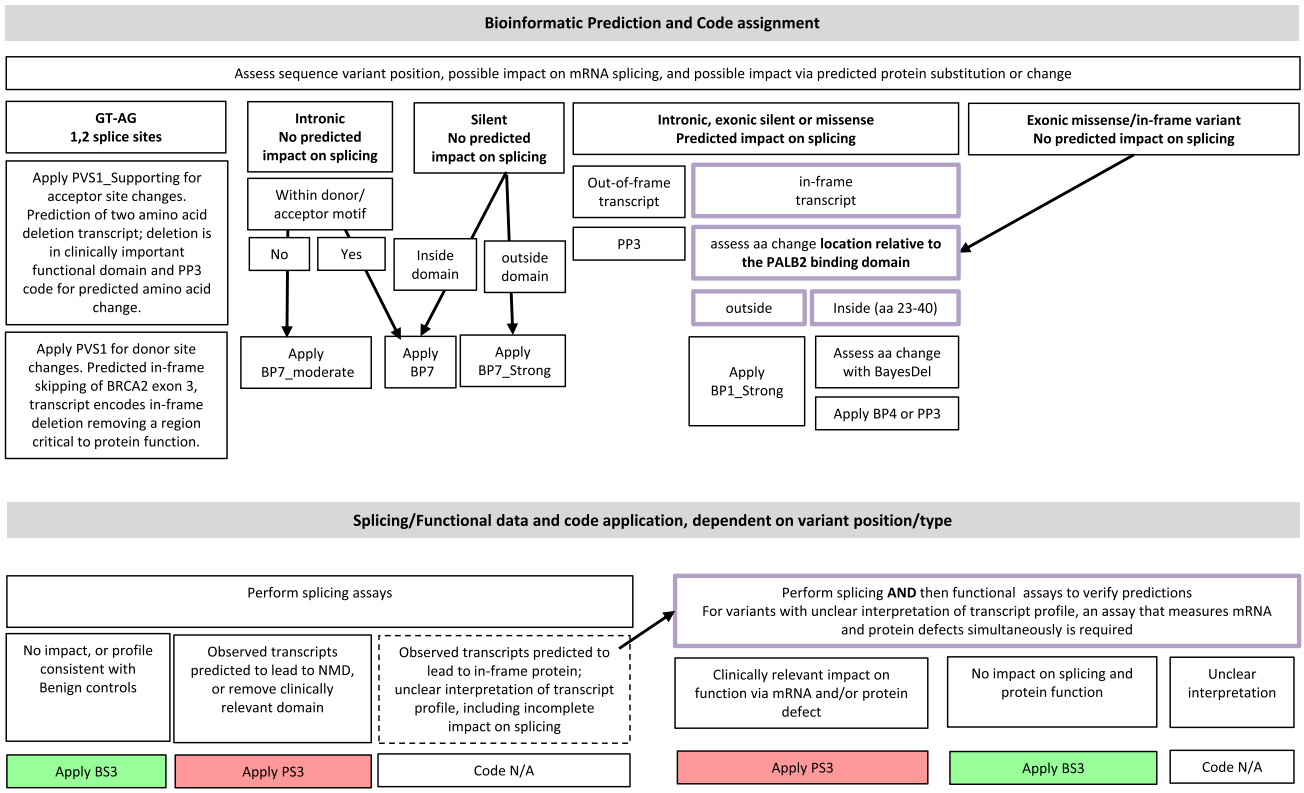

FIGURE 4 Application of codes for variant location relative to functional domain, bioinformatic prediction of effect, and mRNA and/or protein assay data, as applied to variants in/near *BRCA2* exon 3. The donor/acceptor motif location was derived from that of Cartegni et al (Cartegni et al., 2002), namely up to and including the +8 position for the donor motif, and up to and including the −12 position for the acceptor site motif. The PALB2 interaction domain contained within exon 3 was designated conservatively as amino acids (aa) 23–40. Purple border designates variants for which both splicing and functional data are required to consider the assignment of BS3 or PS3 codes. Refer to Section 2 for more detail on level of mRNA aberration and/or functional impact used to assign these codes.

aberrant transcript lacking the six nucleotides in minigene assays, with modest level of ΔE3 also observed for some variants. Similarly, RNA-sequencing analysis of patient material showed a ~3-fold enrichment of transcripts resulting from cryptic splice site usage compared to those due to ΔE3 (Supporting Information: Figure S6c). For c.68-2A>G, both ΔE3 and the 6bp deletion transcript were detected in analysis of mESC RNA (Supporting Information: Figure S8). Variant c.68-2A>G displayed good complementation and HDR capacity of 70%; this finding, together with available clinical evidence against pathogenicity was sufficient to assign a Likely Benign classification. The remaining five possible acceptor site variants are currently considered Uncertain, largely due to lack of information.

Due to inconsistencies in mESC complementation results between this study and that of Tubeuf et al. (2020) for the c.316+6T>A and c.316+6T>G variants (despite roughly concordant levels of ΔE3, accounting for differences in mRNA assay design), functional assay codes were not applied for them. Between-study mESC results were consistent for c.316+6T>C. Considering all applicable codes, c.316+6T>A and c.316+6T>G remained VUS, while c.316+6T>C was classified as Likely Benign.

4 | DISCUSSION

In this study, we used a variety of approaches to calibrate individual evidence types and justify code weights tailored for classification of so-called high-risk pathogenic variants in BRCA1 or BRCA2. We then assessed the utility of these calibrated codes for classification of variants in/near *BRCA2* exon 3, selected as an exemplar for highlighting challenges around interpreting the clinical impact of in-frame deletions (at genomic or mRNA level) that target a known clinically relevant functional domains. Using a points-based (Tavtigian et al., 2020) gene-specific adaptation of the ACMG/AMP criteria, and laboratory assay and clinical data generated from our own work or by previous studies, classification was assigned for 69/85 (81%) of variants in the *BRCA2* exon 3 region (Supporting Information: Table 1). This practical application of the points-based method demonstrated that it was especially beneficial for classification of variants in the benign direction, increasing a class assignment from 49% (42/85) to 81% (69/85). First, the conceptual advantage of the point system is that codes of any strength (for or against pathogenicity) can be combined arithmetically—with a wider range of options for code combinations in the same direction. Notably, it

allows the application of points equivalent to benign moderate, a code that does not exist in the baseline ACMG/AMP system. Further, it simplifies the process for code combinations where evidence may be in the opposing direction, and promotes flexibility to apply additional evidence types in both directions, assuming there is justification for the code strength applied e.g. from clinical calibration. In addition, our study highlights a number of other issues for consideration, as elaborated below.

4.1 | Annotation of splicing predictions—Value and challenges

Our analysis also highlights the importance of careful annotation of predictions for splice site variants, as recommended by Abou Tayoun et al. (2018). All exon 3 splice site variants located at the ±1/2 positions might reasonably have been annotated as PVS1 due to expectation of ΔE3 and in-frame deletion of a clinically important functional domain. However, the cryptic site prediction for the acceptor site variants indicated the possibility of an altered transcript encoding a protein with a two amino acid deletion (p.Asp23_Leu24del), for which there was no existing laboratory evidence for impact on function at the time of our study. Our combined splicing assays showed that all acceptor site variants produced the ΔE3p6 transcript, with modest expression of the ΔE3 for the c.68-2A>G and c.68-1G>A substitutions. Indeed, a recent study (Nix et al., 2021) has highlighted c.68-2A>G as a variant of uncertain clinical significance, on the basis of evidence against pathogenicity derived from an in-house family history weighting algorithm, and detection of the in-frame aberrant transcript in 39% of the total transcript pool for blood-derived mRNA (quantified using a dilution-based method). It is notable that mESC analysis results from our study, which consider impact via mRNA splicing and encoded protein simultaneously, show that the acceptor site variant c.68-2A>G permits complementation, with HDR characteristics of surviving cells consistent with variants categorized as (likely) benign using multifactorial likelihood analysis methodology. Further, the combined clinical data for this variant provided moderate evidence against pathogenicity. Together these findings indicate that the c.68-2A>G variant does not exhibit the functional and clinical features of so-called "high-risk" *BRCA2* variants. We acknowledge that the calibrated evidence types applied here may not reliably detect variants with reduced penetrance relative to the average *BRCA2* premature termination codon variant; alternative analyses, such as large-scale case–control analyses, would be required to assess if c.68-2A>G (and other acceptor site variants) may be associated with low-moderate risk of cancer. We note that this variant is reported 2 times as Likely Pathogenic in Clinvar, based largely on location at a splice site and expectation to cause aberrant splicing and lead to loss of function.

ΔE3 upregulation in at least one assay (>10%) was observed for 11 variants not predicted to affect splicing by our initial MaxEntScan bioinformatic analysis (focused on donor/acceptor loss or donor gain: control variant c.231T>G; c.72_85delinsTTTAAATAGAT; c.91T>C; c.91T>G; c.93G>C; c.93G>T; c.100G>A; c.102A>G; c.316+6T>A; c.316+6T>G; c.316+6T>C. We also reviewed prediction against the SpliceAI tool (Jaganathan et al., 2019) which is becoming more commonly used in the research and clinical setting. Of these, only two were predicted to alter splicing by SpliceAI at a probability threshold of 20% or greater, using the two score approach described in the methods: variant c.316+6T>G with SpliceAI probability of 25% to lead to ΔE3, and demonstrating 77%–88% ΔE3 across multiple assays; variant c.100G>A p.(Glu34Lys) with 20% probability to lead to ΔE3p45, and splicing assays showing variously 14%–57% ΔE3, at higher levels than ΔE3p45 and additional transcripts. These observations suggest that it is appropriately conservative to apply only supporting level of evidence for splicing donor/acceptor loss/gain predictions for variants outside of the consensus site, in the absence of large-scale calibration efforts. Further, it is notable that the vast majority of variants were predicted to alter at least one ESE motif using ESEfinder or RESCUE-ESE (Supporting Information: Table 1), but showed no marked effect on splicing. It is possible that other ESE prediction tools may have better predictive value (Canson et al., 2020), but such analysis was considered outside the scope of this study.

4.2 | Using mRNA and functional assay data from multiple sources—Benefits and challenges

One particularly challenging aspect of this study was interpreting mRNA and functional data generated using a variety of approaches, including use of different mRNA sources and functional assay designs. Moreover, mRNA results were not recorded consistently, with the two main sources of published data presenting findings as % full length relative to WT (Tubeuf et al., 2020), and % canonical and other transcripts in the total transcript pool for an individual (Fraile-Bethencourt et al., 2019). Further, a majority of previous results were generated using RT-PCR methods that can severely overestimate levels of the smaller ΔE3 product; indeed data previously published for LCL-derived mRNA for variant c.68-7>A (Colombo et al., 2018) reports ΔE3 signal to be 33% using RT-PCR versus ~12% using dPCR. To better compare minigene and mESC assay results measuring the effect of a single allele, we calculated an inferred per-allele ΔE3 level for variants assayed using mRNA analysis of patient material. We observed that the ΔE3 level varied somewhat for different blood-related samples, with a tendency for higher ΔE3 level in LCL samples than in other sample types. This was the case for both carrier and noncarrier samples, and the levels correlated across tissue type. For example, c.72_85delinsTTTAAATAGAT showed an inferred per-allele ΔE3 level of 49.2% in LCL-derived mRNA versus 20.8% in mRNA from a PAXgene® sample. Since mRNA analysis results were very reproducible across several technical replicates, and the PAXgene® and LCL samples assayed for the c.72_85delinsTTTAAATAGAT variant were from the same individual, results suggest different absolute level of ΔE3 in different cell types. We thus utilized the ΔE3 levels for known benign variant c.68-7T>A as a strategy to account for differences by sample type.

We also show the importance of using minigene assays, conventional mRNA analysis combined with Sanger sequencing, and RNA-sequencing to detect small changes in mature transcript. Notable examples were detection of the ΔE3p6 transcript (encoding p.Asp23_Leu24del) for the exon 3 acceptor site variants, and detection of ▾E3p2 for variant c.68-3T>G.

Our findings highlight the value of the mESC assay to provide data on both RNA splicing impact and overall functional consequence. While our results indicate similar mRNA transcript expression patterns in mESC and patient samples by dPCR quantitation of ΔE3, the major advantage of this model was that it allowed analysis of the effect of intronic and exonic variants on mRNA splicing in a monoallelic manner. Such effects spanned in-frame exon skipping at various levels and "aberrant" in-frame protein coding events, and transcripts encoding a missense change, or a small in-frame deletion (as observed for c.68-2A>G), and variants that resulted in complex transcript profiles. Despite these advantages, we caution that functional assay methods in general have been calibrated against reference set variants classified using clinical and other features that define them as high-risk pathogenic or not. That is, we cannot exclude the possibility that some variants, in particular those identified as presenting with conflicting results between studies and or other inconsistencies in presentation, may represent hypomorphs potentially associated with reduced (even modest) risk of cancer.

4.3 | Possible future directions arising from laboratory findings

In addition to the important role of functional data in variant classification, the functional data have provided several interesting research questions to be addressed in future studies. Acceptor site variant c.68-2A>G resulted in modest ΔE3 upregulation, and a transcript encoding p.Asp23_Leu24del. In the mESC assay, the same transcripts were expressed, and the overall assay results indicated that the impact of the variant is inconsistent with high risk. This would suggest that amino acids 23 and 24 are not absolutely critical for the PALB2-binding function of this protein domain. Functional data from previous studies (Biswas et al., 2012; Ikegami et al., 2020), and our analysis suggest that p.Trp31 is a critical residue in this domain; c.91T>C (p.Trp31Arg), c.91T>G p.(Trp31Gly), c.93G>C p.(Trp31Cys) and c.93G>T p.(Trp31Cys) demonstrated no/poor complementation in the mESC assay. Indeed, mESC data is in agreement with structural analysis showing that p.Trp31 (but not Asp23 or Leu24) is critical for BRCA2-PALB2 interaction (Oliver et al., 2009), and clinical data reported by Caputo et al. (2021) indicating that c.92G>C p.(Trp31Ser) is associated with high risk of cancer.

Splicing and functional data were thoroughly reviewed to provide insight into the relationship between full-length *BRCA2* transcript expression and protein activity in combination with exon 3 skipping. We have demonstrated the importance of using tissue-matched controls as reference (benign variants known to lead to increased ΔE3, in addition to WT controls) when using nonquantitative or semi-quantitative methods to measure ΔE3. We have also highlighted the need to use quantitative methods to limit the overestimation of ΔE3 levels, to better define the ΔE3 threshold for pathogenicity. We then considered our results in combination with those reported by Tubeuf et al. (2020), with critical examination of the correlation between within-study ΔE3 levels, ΔE3 levels as measured using quantitative dPCR methods in this study, and between-study % survival and results of secondary analysis (Supporting Information: Table 10). Based on quantitative ΔE3 measurement methods, the combined observations suggest that 56% per-allele expression level of ΔE3 (44% WT) for variant c.316+6T>C is sufficient to retain viability (shown by the mESC assay), but ~80% ΔE3 (~20% WT) for the c.316+6T>G and c.316+6T>A variants displays across- and within-study discordant results suggestive of hypomorphic effect (and potentially associated with reduced cancer risk). It will be critical to compile additional clinical data to inform classifications of these variants, and in parallel to consider alternative functional assays that may capture more subtle impacts on function.

4.4 | Independence and application of ACMG/AMP codes, and issues for consideration

We highlight for future discussion issues around independence and application of several ACMG/AMP classification codes. The first question is whether PS3 (Functional studies supportive of damaging effect) should be applied for observation of mRNA results in addition to a relevant PVS1 code for acceptor or donor site variants. Given the extremely high prior probability that a variant altering the highly conserved donor or acceptor site dinucleotide sequence will have an extensive impact on splicing, confirmation of a well-predicted splicing effect adds little information. For example, if an in-frame predicted splicing event is assigned PVS1_Supporting according to the flowchart of Abou Tayoun et al. (2018), then confirmation of such an in-frame event does not alter the uncertainty around whether the in-frame event is important to protein function. Thus, a conservative approach would be to retain the bioinformatic "PVS1" code when confirmed, and simply denote as "confirmed". Further, in the unlikely event that a bioinformatic "PVS1" code is shown to contrast with an experimental result, the reason for the contrasting findings should be used to inform specific and general concepts in derivation of gene-specific PVS1 flowcharts. Given that PS3 is also used to assign results from assays of protein function, or survival assays which measure the effect on combined mRNA and protein, perhaps it would be simpler to retain PS3 only for application of "functional assays" that capture more than mRNA splicing, since as shown here they can provide additional information to that from mRNA splicing results. The second question is whether it is double-counting to apply PS1 (Splicing) on the basis of similarity to prediction for a known pathogenic variant at the same position. We argue not, since the rationale for applying the PS1 (Splicing) code is - as for the baseline

PS1 missense code - that the clinical information for a pathogenic variant can be "borrowed" as evidence to classify a second variant, for which pathogenicity is assumed to be due to the same molecular mechanism. The use of a PS1 (Splicing) code is particularly important for variants outside of the donor and acceptor sites, with a starting bioinformatic code at only supporting level. We also raise for debate whether the same concept should be introduced as a new ACMG/AMP code as evidence against pathogenicity. That is, if a variant with no prediction to alter a missense or splicing profile is classified as benign using clinical and other data, then another variant with the same bioinformatics scores could be assumed also to have no molecular and clinical impact on disease risk. In addition, we show here how missense variant location outside a domain provides valuable evidence against pathogenicity, irrespective of bioinformatic prediction of missense effect. Conceptually this is not new, and has been captured as low prior probability of pathogenicity for *BRCA1* and *BRCA2* multifactorial likelihood analysis (Easton et al., 2007; Li et al., 2020); we assigned this evidence type as BP1_Strong, since it is not captured in the baseline ACMG-AMP criteria.

5 | CONCLUSIONS

There were three main messages arising from this study. First, annotation of donor and acceptor sites requires careful consideration of cryptic splice site usage and critical domain knowledge to appropriately assign PVS1 code strength. Second, splicing assays have great utility for functional assessment of intronic and synonymous variants, but genomic-based functional assays that capture both mRNA and protein effects provide critical findings for the assessment of variants leading to transcript profiles of uncertain significance, including those encoding a missense change/s. Third, statistically derived odds and LRs for variant pathogenicity assessment, derived for a range of data types, show great utility in a gene-specific points-based application of ACMG/AMP guidelines.

ACKNOWLEDGMENTS

The authors thank J. Jonkers and P. Bouwman (Netherlands Cancer Institute, Amsterdam, the Netherlands) for the I-Sce1-mCherry plasmid; S.K. Sharan (National Cancer Institute at Frederick, Frederick, USA) for the PI2F7 conditional Brca2 knockout mES cell line (PMID: 18607349); M. Jasin (Memorial Sloan-Kettering Cancer Center, New York, USA) for the DR-GFP reporter plasmid (PMID: 11239455). The authors wish also to thank all the members of the ICO Hereditary Cancer Program. LCW was supported by the Royal Society of New Zealand Rutherford Discovery Fellowship. The FPGMX thanks members of the Cancer Genetics group (IDIS): Miguel Aguado, Olivia Fuentes, and Ana Crujeiras. The work of MPGV was financially supported by the Dutch Cancer Society KWF (UL2012-5649 and Pink Ribbon-11704). The work by PM was supported by a "Pink Ribbon" grant #194751 from Den Norske Kreftforening to E.H. The work of MdlH was supported by Spanish Instituto de Salud Carlos III (ISCIII) funding grant PI 20/00110, an initiative of the Spanish Ministry of Economy and Innovation. ABS, MTP and ET were supported by NHMRC Funding (APP177524, APP1104808). The work by CL and MM received institutional support by CERCA Program/Generalitat de Catalunya and grant support by the Carlos III National Health Institute funded by FEDER funds—a way to build Europe—[PI19/00553; PI16/00563; SAF2015-68016-R and CIBERONC]; the Government of Catalonia [Pla estratègic de recerca i innovació en salut (PERIS_MedPerCan and URDCat projects), 2017SGR1282 and 2017SGR496]. The Baralle lab is supported by NIHR Research Professorship to DB (RP-2016-07-011). The work of AV was supported by the Spanish Health Research Foundation, Instituto de Salud Carlos III (ISCIII) through Research Activity Intensification Program (contract grant numbers: INT15/00070, INT16/00154, INT17/00133, and INT20/00071), and through Centro de Investigación Biomédica en Red de Enfermedades Raras CIBERER (ACCI 2016: ER17P1AC7112/2018); Autonomous Government of Galicia (Consolidation and structuring program: IN607B), and by the Fundación Mutua Madrileña (call 2018). The German Consortium of Hereditary Breast and Ovarian Cancer (GC-HBOC) is supported by the German Cancer Aid (Grant nos. 110837 and 70114178), (RKS) and by the Federal Ministry of Education and Research (Grant no. 01GY1901), (RKS). The work of EMA was supported by the Ministry of Health of the Czech Republic MH CZ—DRO (MMCI, 00209805) and AZV project NU20-03-00285. Institutional support by Italian Ministy of Health, Ricerca Corrente of CRO Aviano, Line 1 (AVI).

CONFLICTS OF INTEREST

The PERCH software, for which BJ Feng is the inventor, has been non-exclusively licensed to Ambry Genetics Corporation for their clinical genetic testing services and research. Dr. Feng also reports funding and sponsorship to his institution on his behalf from Pfizer Inc., Regeneron Genetics Center LLC., and Astra Zeneca. TvOH has received lecture honoraria from Pfizer. Nelly Abualkheir, Blair R. Conner, Lily Hoang, Rachid Karam, Holly LaDuca, Tina Pesaran, and Marcy E. Richardson are paid employees of Ambry Genetics. All other authors have declared no conflicts of interest.

ORCID

Mads Thomassen http://orcid.org/0000-0003-0078-1217
Romy L. S. Mesman https://orcid.org/0000-0001-9783-7138
Emma Tudini http://orcid.org/0000-0002-5834-7862
Michael T. Parsons http://orcid.org/0000-0003-3242-8477
Brage S. Andresen http://orcid.org/0000-0001-7488-3035
Rachid Karam http://orcid.org/0000-0002-5645-498X
Paul A. James http://orcid.org/0000-0002-4361-4657
David E. Goldgar http://orcid.org/0000-0003-0697-9347
Logan C. Walker http://orcid.org/0000-0003-0018-3719
Kathleen B. M. Claes http://orcid.org/0000-0003-0841-7372
Diana Baralle http://orcid.org/0000-0002-3560-6980
Ana Vega http://orcid.org/0000-0002-7416-5137
Maaike P. G. Vreeswijk http://orcid.org/0000-0003-4068-9271
Miguel de la Hoya http://orcid.org/0000-0002-8113-1410
Amanda B. Spurdle http://orcid.org/0000-0003-1337-7897

REFERENCES

Abou Tayoun, A. N., Pesaran, T., DiStefano, M. T., Oza, A., Rehm, H. L., Biesecker, L. G., & Harrison, S. M. (2018). Recommendations for interpreting the loss of function PVS1 ACMG/AMP variant criterion. *Human Mutation*, *39*(11), 1517–1524. https://doi.org/10.1002/humu.23626

Biswas, K., Das, R., Eggington, J. M., Qiao, H., North, S. L., Stauffer, S., Burkett, S. S., Martin, B. K., Southon, E., Sizemore, S. C., Pruss, D., Bowles, K. R., Roa, B. B., Hunter, N., Tessarollo, L., Wenstrup, R. J., Byrd, R. A., & Sharan, S. K. (2012). Functional evaluation of BRCA2 variants mapping to the PALB2-binding and C-terminal DNA-binding domains using a mouse ES cell-based assay. *Human Molecular Genetics*, *21*(18), 3993–4006. https://doi.org/10.1093/hmg/dds222

Canson, D., Glubb, D., & Spurdle, A. B. (2020). Variant effect on splicing regulatory elements, branchpoint usage, and pseudoexonization: Strategies to enhance bioinformatic prediction using hereditary cancer genes as exemplars. *Human Mutation*, *41*(10), 1705–1721. https://doi.org/10.1002/humu.24074

Caputo, S., Telly, D., Briaux, A., Sesen, J., Ceppi, M., Bonnet, F., Bourdon, V., Coulet, F., Castera, L., Delnatte, C., Hardouin, A., Mazoyer, S., Schultz, I., Sevenet, N., Uhrhammer, N., Bonnet, C., Tilkin-Mariamé, A. F., Houdayer, C., Moncoutier, V., … Rouleau, E. (2021). 5' Region large genomic rearrangements in the BRCA1 gene in French families: Identification of a tandem triplication and nine distinct deletions with five recurrent breakpoints. *Cancers*, *13*(13):3171. https://doi.org/10.3390/cancers13133171

Caputo, S. M., Léone, M., Damiola, F., Ehlen, A., Carreira, A., Gaidrat, P., Martins, A., Brandão, R. D., Peixoto, A., Vega, A., Houdayer, C., Delnatte, C., Bronner, M., Muller, D., Castera, L., Guillaud-Bataille, M., Søkilde, I., Uhrhammer, N., Demontety, S., … Rouleau, E. (2018). Full in-frame exon 3 skipping of BRCA2 confers high risk of breast and/or ovarian cancer. *Oncotarget*, *9*(25), 17334–17348. https://doi.org/10.18632/oncotarget.24671

Cartegni, L., Chew, S. L., & Krainer, A. R. (2002). Listening to silence and understanding nonsense: Exonic mutations that affect splicing. *Nature Reviews Genetics*, *3*(4), 285–298. https://doi.org/10.1038/nrg775

Colombo, M., Lòpez-Perolio, I., Meeks, H. D., Caleca, L., Parsons, M. T., Li, H., De Vecchi, G., Tudini, E., Foglia, C., Mondini, P., Manoukian, S., Behar, R., Garcia, E. B. G., Meindl, A., Montagna, M., Niederacher, D., Schmidt, A. Y., Varesco, L., Wappenschmidt, B., … Radice, P. (2018). The BRCA2 c.68-7T > A variant is not pathogenic: A model for clinical calibration of spliceogenicity. *Human Mutation*, *39*, 729–741. https://doi.org/10.1002/humu.23411

Conner, B. R., Hernandez, F., Souders, B., Landrith, T., Boland, C. R., & Karam, R. (2019). RNA analysis identifies pathogenic duplications in MSH2 in patients with lynch syndrome. *Gastroenterology*, *156*(6), 1924–1925. https://doi.org/10.1053/j.gastro.2019.01.248

Diez, O., Gutierrez-Enriquez, S., Ramon y Cajal, T., Alonso, C., Balmana, J., & Llort, G. (2007). Caution should be used when interpreting alterations affecting the exon 3 of the BRCA2 gene in breast/ovarian cancer families. *Journal of Clinical Oncology*, *25*(31), 5035–5036. https://doi.org/10.1200/JCO.2007.13.4346

Dines, J. N., Shirts, B. H., Slavin, T. P., Walsh, T., King, M. C., Fowler, D. M., & Pritchard, C. C. (2020). Systematic misclassification of missense variants in BRCA1 and BRCA2 "coldspots". *Genetics in Medicine*, *22*(5), 825–830. https://doi.org/10.1038/s41436-019-0740-6

Dorling, L., Carvalho, S., Allen, J., González-Neira, A., Luccarini, C., Wahlström, C., Pooley, K. A., Parsons, M. T., Fortuno, C., Wang, Q., Bolla, M. K., Dennis, J., Keeman, R., Alonso, M. R., Álvarez, N., Herraez, B., Fernandez, V., Núñez-Torres, R., Osorio, A., … Rookus, M. A. (2021). Breast cancer risk genes – Association analysis in more than 113,000 women. *New England Journal of Medicine*, *384*(5), 428–439. https://doi.org/10.1056/NEJMoa1913948

Easton, D. F., Deffenbaugh, A. M., Pruss, D., Frye, C., Wenstrup, R. J., Allen-Brady, K., Tavtigian, S. V., Monteiro, A. N., Iversen, E. S., Couch, F. J., & Goldgar, D. E. (2007). A systematic genetic assessment of 1,433 sequence variants of unknown clinical significance in the BRCA1 and BRCA2 breast cancer-predisposition genes. *American Journal of Human Genetics*, *81*(5), 873–883. https://doi.org/10.1086/521032

Fackenthal, J. D., Yoshimatsu, T., Zhang, B., de Garibay, G. R., Colombo, M., De Vecchi, G., Ayoub, S. C., Lal, K., Olopade, O. I., Vega, A., Santamariña, M., Blanco, A., Wappenschmidt, B., Becker, A., Houdayer, C., Walker, L. C., López-Perolio, I., Thomassen, M., Parsons, M., … de la Hoya, M. (2016). Naturally occurring BRCA2 alternative mRNA splicing events in clinically relevant samples. *Journal of Medical Genetics*, *53*(8), 548–558. https://doi.org/10.1136/jmedgenet-2015-103570

Farber-Katz, S., Hsuan, V., Wu, S., Landrith, T., Vuong, H., Xu, D., Li, B., Hoo, J., Lam, S., Nashed, S., Toppmeyer, D., Gray, P., Haynes, G., Lu, H. M., Elliott, A., Tippin Davis, B., & Karam, R. (2018). Quantitative analysis of BRCA1 and BRCA2 germline splicing variants using a novel RNA-massively parallel sequencing assay. *Frontiers in Oncology*, *8*, 286. https://doi.org/10.3389/fonc.2018.00286

Fraile-Bethencourt, E., Valenzuela-Palomo, A., Diez-Gomez, B., Goina, E., Acedo, A., Buratti, E., & Velasco, E. A. (2019). Mis-splicing in breast cancer: Identification of pathogenic BRCA2 variants by systematic minigene assays. *Journal of Pathology*, *248*(4), 409–420. https://doi.org/10.1002/path.5268

de Garibay, G. R., Acedo, A., García-Casado, Z., Gutiérrez-Enríquez, S., Tosar, A., Romero, A., Garre, P., Llort, G., Thomassen, M., Díez, O., Pérez-Segura, P., Díaz-Rubio, E., Velasco, E. A., Caldés, T., & de la Hoya, M. (2014). Capillary electrophoresis analysis of conventional splicing assays: IARC analytical and clinical classification of 31 BRCA2 genetic variants. *Human Mutation*, *35*(1), 53–57. https://doi.org/10.1002/humu.22456

Gayther, S. A., Mangion, J., Russell, P., Seal, S., Barfoot, R., Ponder, B. A., Stratton, M. R., & Easton, D. (1997). Variation of risks of breast and ovarian cancer associated with different germline mutations of the BRCA2 gene. *Nature Genetics*, *15*(1), 103–105. https://doi.org/10.1038/ng0197-103

Goldgar, D. E., Easton, D. F., Byrnes, G. B., Spurdle, A. B., Iversen, E. S., Greenblatt, M. S., & IARC Unclassified Genetic Variants Working Group. (2008). Genetic evidence and integration of various data sources for classifying uncertain variants into a single model. *Human Mutation*, *29*(11), 1265–1272. https://doi.org/10.1002/humu.20897

Goldgar, D. E., Easton, D. F., Deffenbaugh, A. M., Monteiro, A. N., Tavtigian, S. V., Couch, F. J., & Breast Cancer Information Core Steering, C. (2004). Integrated evaluation of DNA sequence variants of unknown clinical significance: Application to BRCA1 and BRCA2. *American Journal of Human Genetics*, *75*(4), 535–544. https://doi.org/10.1086/424388

Guidugli, L., Shimelis, H., Masica, D. L., Pankratz, V. S., Lipton, G. B., Singh, N., Hu, C., Monteiro, A., Lindor, N. M., Goldgar, D. E., Karchin, R., Iversen, E. S., & Couch, F. J. (2018). Assessment of the clinical relevance of BRCA2 missense variants by functional and computational approaches. *American Journal of Human Genetics*, *102*, 233–248. https://doi.org/10.1016/j.ajhg.2017.12.013

Hartford, S. A., Chittela, R., Ding, X., Vyas, A., Martin, B., Burkett, S., Haines, D. C., Southon, E., Tessarollo, L., & Sharan, S. K. (2016). Interaction with PALB2 is essential for maintenance of genomic integrity by BRCA2. *PLoS Genetics*, *12*(8):e1006236. https://doi.org/10.1371/journal.pgen.1006236

de la Hoya, M., Soukarieh, O., López-Perolio, I., Vega, A., Walker, L. C., van Ierland, Y., Baralle, D., Santamariña, M., Lattimore, V., Wijnen, J., Whiley, P., Blanco, A., Raponi, M., Hauke, J., Wappenschmidt, B.,

Becker, A., Hansen, T. V., Behar, R., Investigators, K., … Spurdle, A. B. (2016). Combined genetic and splicing analysis of BRCA1 c.[594-2A>C; 641A>G] highlights the relevance of naturally occurring in-frame transcripts for developing disease gene variant classification algorithms. *Human Molecular Genetics*, *25*(11), 2256–2268. https://doi.org/10.1093/hmg/ddw094

http://agvgd.hci.utah.edu/

http://fengbj-laboratory.org/BayesDel/BayesDel.html

https://spliceailookup.broadinstitute.org

http://varnomen.hgvs.org/

Ikegami, M., Kohsaka, S., Ueno, T., Momozawa, Y., Inoue, S., Tamura, K., Shimomura, A., Hosoya, N., Kobayashi, H., Tanaka, S., & Mano, H. (2020). High-throughput functional evaluation of BRCA2 variants of unknown significance. *Nature Communications*, *11*(1), 2573. https://doi.org/10.1038/s41467-020-16141-8

Jaganathan, K., Kyriazopoulou Panagiotopoulou, S., McRae, J. F., Darbandi, S. F., Knowles, D., Li, Y. I., Kosmicki, J. A., Arbelaez, J., Cui, W., Schwartz, G. B., Chow, E. D., Kanterakis, E., Gao, H., Kia, A., Batzoglou, S., Sanders, S. J., & Farh, K. K. (2019). Predicting splicing from primary sequence with deep learning. *Cell*, *176*(3), 535–548. https://doi.org/10.1016/j.cell.2018.12.015

Landrith, T., Li, B., Cass, A. A., Conner, B. R., LaDuca, H., McKenna, D. B., Maxwell, K. N., Domchek, S., Morman, N. A., Heinlen, C., Wham, D., Koptiuch, C., Vagher, J., Rivera, R., Bunnell, A., Patel, G., Geurts, J. L., Depas, M. M., Gaonkar, S., … Karam, R. (2020). Splicing profile by capture RNA-seq identifies pathogenic germline variants in tumor suppressor genes. *npj Precision Oncology*, *4*, 4. https://doi.org/10.1038/s41698-020-0109-y

Li, H., LaDuca, H., Pesaran, T., Chao, E. C., Dolinsky, J. S., Parsons, M., Spurdle, A. B., Polley, E. C., Shimelis, H., Hart, S. N., Hu, C., Couch, F. J., & Goldgar, D. E. (2020). Classification of variants of uncertain significance in BRCA1 and BRCA2 using personal and family history of cancer from individuals in a large hereditary cancer multigene panel testing cohort. *Genetics in Medicine*, *22*(4), 701–708. https://doi.org/10.1038/s41436-019-0729-1

Mesman, R., Calléja, F., Hendriks, G., Morolli, B., Misovic, B., Devilee, P., van Asperen, C. J., Vrieling, H., & Vreeswijk, M. (2019). The functional impact of variants of uncertain significance in BRCA2. *Genetics in Medicine*, *21*(2), 293–302. https://doi.org/10.1038/s41436-018-0052-2

Mesman, R. L. S., Calleja, F., de la Hoya, M., Devilee, P., van Asperen, C. J., Vrieling, H., & Vreeswijk, M. P. G. (2020). Alternative mRNA splicing can attenuate the pathogenicity of presumed loss-of-function variants in BRCA2. *Genetics in Medicine*, *22*(8), 1355–1365. https://doi.org/10.1038/s41436-020-0814-5

Mohammadi, L., Vreeswijk, M. P., Oldenburg, R., van den Ouweland, A., Oosterwijk, J. C., van der Hout, A. H., Hoogerbrugge, N., Ligtenberg, M., Ausems, M. G., van der Luijt, R. B., Dommering, C. J., Gille, J. J., Verhoef, S., Hogervorst, F. B., van Os, T. A., Gómez García, E., Blok, M. J., Wijnen, J. T., Helmer, Q., … van Houwelingen, H. C. (2009). A simple method for co-segregation analysis to evaluate the pathogenicity of unclassified variants; BRCA1 and BRCA2 as an example. *BMC Cancer*, *9*, 211. https://doi.org/10.1186/1471-2407-9-211

Montalban, G., Fraile-Bethencourt, E., López-Perolio, I., Pérez-Segura, P., Infante, M., Durán, M., Alonso-Cerezo, M. C., López-Fernández, A., Diez, O., de la Hoya, M., Velasco, E. A., & Gutiérrez-Enríquez, S. (2018). Characterization of spliceogenic variants located in regions linked to high levels of alternative splicing: BRCA2 c.7976+5G > T as a case study. *Human Mutation*, *39*(9), 1155–1160. https://doi.org/10.1002/humu.23583

Nacson, J., Di Marcantonio, D., Wang, Y., Bernhardy, A. J., Clausen, E., Hua, X., Cai, K. Q., Martinez, E., Feng, W., Callén, E., Wu, W., Gupta, G. P., Testa, J. R., Nussenzweig, A., Sykes, S. M., & Johnson, N. (2020). BRCA1 mutational complementation induces synthetic viability. *Molecular Cell*, *78*(5), 951–959. https://doi.org/10.1016/j.molcel.2020.04.006

Nix, P., Mundt, E., Coffee, B., Goossen, E., Warf, B. M., Brown, K., Bowles, K., & Roa, B. (2021). Interpretation of BRCA2 splicing variants: A case series of challenging variant interpretations and the importance of functional RNA analysis. *Familial Cancer*, *21*, 7–19. https://doi.org/10.1007/s10689-020-00224-y

Nordling, M., Karlsson, P., Wahlstrom, J., Engwall, Y., Wallgren, A., & Martinsson, T. (1998). A large deletion disrupts the exon 3 transcription activation domain of the BRCA2 gene in a breast/ovarian cancer family. *Cancer Research*, *58*(7), 1372–1375.

Oliver, A. W., Swift, S., Lord, C. J., Ashworth, A., & Pearl, L. H. (2009). Structural basis for recruitment of BRCA2 by PALB2. *EMBO Reports*, *10*(9), 990–996. https://doi.org/10.1038/embor.2009.126

Parsons, M. T., Tudini, E., Li, H., Hahnen, E., Wappenschmidt, B., Feliubadaló, L., Aalfs, C. M., Agata, S., Aittomäki, K., Alducci, E., Alonso-Cerezo, M. C., Arnold, N., Auber, B., Austin, R., Azzollini, J., Balmaña, J., Barbieri, E., Bartram, C. R., Blanco, A., … Pohl-Rescigno, E. (2019). Large scale multifactorial likelihood quantitative analysis of BRCA1 and BRCA2 variants: An ENIGMA resource to support clinical variant classification. *Human Mutation*, *40*(9), 1557–1578. https://doi.org/10.1002/humu.23818

Peixoto, A., Santos, C., Rocha, P., Pinheiro, M., Príncipe, S., Pereira, D., Rodrigues, H., Castro, F., Abreu, J., Gusmão, L., Amorim, A., & Teixeira, M. R. (2009). The c.156_157insAlu BRCA2 rearrangement accounts for more than one-fourth of deleterious BRCA mutations in northern/central Portugal. *Breast Cancer Research and Treatment*, *114*(1), 31–38. https://doi.org/10.1007/s10549-008-9978-4

Richards, S., Aziz, N., Bale, S., Bick, D., Das, S., Gastier-Foster, J., Grody, W. W., Hegde, M., Lyon, E., Spector, E., Voelkerding, K., Rehm, H. L., & ACMG Laboratory Quality Assurance, C. (2015). Standards and guidelines for the interpretation of sequence variants: A joint consensus recommendation of the American College of Medical Genetics and Genomics and the Association for Molecular Pathology. *Genetics in Medicine*, *17*(5), 405–424. https://doi.org/10.1038/gim.2015.30

Sanz, D. J., Acedo, A., Infante, M., Durán, M., Pérez-Cabornero, L., Esteban-Cardeñosa, E., Lastra, E., Pagani, F., Miner, C., & Velasco, E. A. (2010). A high proportion of DNA variants of BRCA1 and BRCA2 is associated with aberrant splicing in breast/ovarian cancer patients. *Clinical Cancer Research*, *16*(6), 1957–1967. https://doi.org/10.1158/1078-0432.CCR-09-2564

Shamsani, J., Kazakoff, S. H., Armean, I. M., McLaren, W., Parsons, M. T., Thompson, B. A., O'Mara, T. A., Hunt, S. E., Waddell, N., & Spurdle, A. B. (2019). A plugin for the ensembl variant effect predictor that uses MaxEntScan to predict variant spliceogenicity. *Bioinformatics*, *35*(13), 2315–2317. https://doi.org/10.1093/bioinformatics/bty960

Spurdle, A. B., Couch, F. J., Parsons, M. T., McGuffog, L., Barrowdale, D., Bolla, M. K., Wang, Q., Healey, S., Schmutzler, R., Wappenschmidt, B., Rhiem, K., Hahnen, E., Engel, C., Meindl, A., Ditsch, N., Arnold, N., Plendl, H., Niederacher, D., Sutter, C., … Henderson, B. E. (2014). Refined histopathological predictors of BRCA1 and BRCA2 mutation status: a large-scale analysis of breast cancer characteristics from the BCAC, CIMBA, and ENIGMA consortia. *Breast Cancer Research*, *16*(6):3419. https://doi.org/10.1186/s13058-014-0474-y

Spurdle, A. B., Healey, S., Devereau, A., Hogervorst, F. B., Monteiro, A. N., Nathanson, K. L., Radice, P., Stoppa-Lyonnet, D., Tavtigian, S., Wappenschmidt, B., Couch, F. J., & Goldgar, D. E., ENIGMA. (2012). ENIGMA—Evidence-based network for the interpretation of germline mutant alleles: an international initiative to evaluate risk and clinical significance associated with sequence variation in BRCA1 and BRCA2 genes. *Human Mutation*, *33*(1), 2–7. https://doi.org/10.1002/humu.21628

Sy, S. M., Huen, M. S., & Chen, J. (2009). PALB2 is an integral component of the BRCA complex required for homologous recombination repair. *Proceedings of the National Academy of Sciences of the United States of America*, *106*(17), 7155–7160. https://doi.org/10.1073/pnas.0811159106

Tavtigian, S. V., Byrnes, G. B., Goldgar, D. E., & Thomas, A. (2008). Classification of rare missense substitutions, using risk surfaces, with genetic- and molecular-epidemiology applications. *Human Mutation*, *29*(11), 1342–1354. https://doi.org/10.1002/humu.20896

Tavtigian, S. V., Greenblatt, M. S., Harrison, S. M., Nussbaum, R. L., Prabhu, S. A., Boucher, K. M., Biesecker, L. G., & ClinGen Sequence Variant Interpretation Working Group (ClinGen SVI). (2018). Modeling the ACMG/AMP variant classification guidelines as a Bayesian classification framework. *Genetics in Medicine*, *20*(9), 1054–1060. https://doi.org/10.1038/gim.2017.210

Tavtigian, S. V., Harrison, S. M., Boucher, K. M., & Biesecker, L. G. (2020). Fitting a naturally scaled point system to the ACMG/AMP variant classification guidelines. *Human Mutation*, *41*, 1734–1737. https://doi.org/10.1002/humu.24088

Thomassen, M., Blanco, A., Montagna, M., Hansen, T. V., Pedersen, I. S., Gutiérrez-Enríquez, S., Menéndez, M., Fachal, L., Santamariña, M., Steffensen, A. Y., Jønson, L., Agata, S., Whiley, P., Tognazzo, S., Tornero, E., Jensen, U. B., Balmaña, J., Kruse, T. A., Goldgar, D. E., … Vega, A. (2012). Characterization of BRCA1 and BRCA2 splicing variants: A collaborative report by ENIGMA consortium members. *Breast Cancer Research and Treatment*, *132*(3), 1009–1023. https://doi.org/10.1007/s10549-011-1674-0

Thompson, D., Easton, D. F., & Goldgar, D. E. (2003). A full-likelihood method for the evaluation of causality of sequence variants from family data. *American Journal of Human Genetics*, *73*(3), 652–655. https://doi.org/10.1086/378100

Tubeuf, H., Caputo, S. M., Sullivan, T., Rondeaux, J., Krieger, S., Caux-Moncoutier, V., Hauchard, J., Castelain, G., Fiévet, A., Meulemans, L., Révillion, F., Léoné, M., Boutry-Kryza, N., Delnatte, C., Guillaud-Bataille, M., Cleveland, L., Reid, S., Southon, E., Soukarieh, O., … Martins, A. (2020). Calibration of pathogenicity due to variant-induced leaky splicing defects by using BRCA2 exon 3 as a model system. *Cancer Research*, *80*(17), 3593–3605. https://doi.org/10.1158/0008-5472.CAN-20-0895

Valenzuela-Palomo, A., Bueno-Martínez, E., Sanoguera-Miralles, L., Lorca, V., Fraile-Bethencourt, E., Esteban-Sánchez, A., Gómez-Barrero, S., Carvalho, S., Allen, J., García-Álvarez, A., Pérez-Segura, P., Dorling, L., Easton, D. F., Devilee, P., Vreeswijk, M. P., de la Hoya, M., & Velasco, E. A. (2022). Splicing predictions, minigene analyses, and ACMG-AMP clinical classification of 42 germline PALB2 splice-site variants. *Journal of Pathology*, *256*(3), 321–334. https://doi.org/10.1002/path.5839

Xia, B., Sheng, Q., Nakanishi, K., Ohashi, A., Wu, J., Christ, N., Liu, X., Jasin, M., Couch, F. J., & Livingston, D. M. (2006). Control of BRCA2 cellular and clinical functions by a nuclear partner, PALB2. *Molecular Cell*, *22*(6), 719–729. https://doi.org/10.1016/j.molcel.2006.05.022

Yeo, G., & Burge, C. B. (2004). Maximum entropy modeling of short sequence motifs with applications to RNA splicing signals. *Journal of Computational Biology*, *11*(2–3), 377–394. https://doi.org/10.1089/1066527041410418

SUPPORTING INFORMATION

Additional supporting information can be found online in the Supporting Information section at the end of this article.

How to cite this article: Thomassen, M., Mesman, R. L. S., Hansen, T. V. O., Menendez, M., Rossing, M., Esteban-Sánchez, A., Tudini, E., Törngren, T., Parsons, M. T., Pedersen, I. S., Teo, S. H., Kruse, T. A., Møller, P., Borg, Å., Jensen, U. B., Christensen, L. L., Singer, C. F., Muhr, D., Santamarina, M., … Spurdle, A. B. (2022). Clinical, splicing, and functional analysis to classify *BRCA2* exon 3 variants: Application of a points-based ACMG/AMP approach. *Human Mutation*, 43, 1921–1944. https://doi.org/10.1002/humu.24449